Differential Occurrence of Reluctant Openings in G-Protein–inhibited N- and P/Q-type Calcium Channels

Henry M. Colecraft, Parag G. Patil, and David T. Yue

From the Program in Molecular and Cellular Systems Physiology, Departments of Biomedical Engineering and Neuroscience, Johns Hopkins University School of Medicine, Baltimore, Maryland 21205

abstract Voltage-dependent inhibition of N- and P/Q-type calcium channels by G proteins is crucial for presynaptic inhibition of neurotransmitter release, and may contribute importantly to short-term synaptic plasticity. Such calcium-channel modulation could thereby impact significantly the neuro-computational repertoire of neural networks. The differential modulation of N and P/Q channels could even further enrich their impact upon synaptic tuning. Here, we performed in-depth comparison of the G-protein inhibition of recombinant N and P/Q channels, expressed in HEK 293 cells with the m2 muscarinic receptor. While both channel types display classic features of G-protein modulation (kinetic slowing of activation, prepulse facilitation, and voltage dependence of inhibition), we confirmed previously reported quantitative differences, with N channels displaying stronger inhibition and greater relief of inhibition by prepulses. A more fundamental, qualitative difference in the modulation of these two channels was revealed by a modified tail-activation paradigm, as well as by a novel "slope" analysis method comparing time courses of slow activation and prepulse facilitation. The stark contrast in modulatory behavior can be understood within the context of the "willing–reluctant" model, in which binding of G-protein βγ subunits to channels induces a reluctant mode of gating, where stronger depolarization is required for opening. Our experiments suggest that only N channels could be opened in the reluctant mode, at voltages normally spanned by neuronal action potentials. By contrast, P/Q channels appear to remain closed, especially over these physiological voltages. Further, the differential occurrence of reluctant openings is not explained by differences in the rate of G-protein unbinding from the two channels. These two scenarios predict very different effects of G-protein inhibition on the waveform of Ca^{2+} entry during action potentials, with potentially important consequences for the timing and efficacy of synaptic transmission.

key words: α_{1A} • α_{1B} • channel modulation • heterologous expression • short-term synaptic plasticity

INTRODUCTION

High voltage-activated calcium channels (N, L, P/Q and R type) are present in central and peripheral neurons, where they gate Ca^{2+} influx to mediate and regulate such essential Ca^{2+}-dependent processes as gene expression, membrane excitability, and synaptic transmission (Tsien and Tsien, 1990; Bito et al., 1997). In tune with their vital role in cellular control, calcium channels are modulated by an array of intracellular signaling pathways, providing powerful means to fine tune biological function by controlling Ca^{2+} influx.

One important and widespread form of calcium channel modulation is voltage-dependent inhibition of N- and P/Q-type channels by receptor-coupled, heterotrimeric G proteins (Wanke et al., 1987; Ikeda and Schofield, 1989; Lipscombe et al., 1989; Elmslie et al., 1990; Zhu and Ikeda, 1994). Direct binding of G-protein βγ subunits ($G_{\beta\gamma}$)[1] to distinct domains on the channels is thought to produce the channel inhibition (Herlitze et al., 1996; Ikeda, 1996; Zhang et al., 1996; De Waard et al., 1997; Qin et al., 1997; Zamponi et al., 1997; Furukawa et al., 1998a,b; Zamponi and Snutch, 1998; Canti et al., 1999). As N- and P/Q-type channels figure prominently in triggering neurotransmitter release (Luebke et al., 1993; Takahashi and Momiyama, 1993; Wheeler et al., 1994; Wu and Saggau, 1994; Reid et al., 1998), this type of modulation is a dominant mechanism for presynaptic inhibition of synaptic transmission (Wu and Saggau, 1997). Such modulation may also contribute to short-term synaptic plasticity by virtue of the transient relief of G-protein inhibition with depolarization (Elmslie et al., 1990; Miller, 1990; Wu and Saggau, 1994; Dittman and Regehr, 1996; Brody et al., 1997; Brody and Yue, 1999). Even more intriguing is the potential for differential G-protein modulation of N- and P/Q-type channels to produce selective regulation of synaptic efficacy at spatially distinct sites, as varying proportions of N- and P/Q-type channels mediate

Address correspondence to David T. Yue, Program in Molecular and Cellular Systems Physiology, Departments of Biomedical Engineering and Neuroscience, Johns Hopkins University School of Medicine, Ross Building, Room 713, 720 Rutland Avenue, Baltimore, MD 21205. Fax: 410-955-0549; E-mail: dyue@bme.jhu.edu

[1]*Abbreviations used in this paper:* CCh, carbachol; $G_{\beta\gamma}$, G-protein βγ subunits.

J. Gen. Physiol. © The Rockefeller University Press • 0022-1295/2000/02/175/18 $5.00
Volume 115 February 2000 175–192
Released online 31 January 2000
http://www.jgp.org

synaptic transmission at different synapses (Luebke et al., 1993; Takahashi and Momiyama, 1993; Wheeler et al., 1994; Wu and Saggau, 1994; Reid et al., 1998). In fact, some quantitative differences in the strength of G-protein modulation of N- and P/Q-type channels have been documented (Mintz and Bean, 1993; Bourinet et al., 1996; Zhang et al., 1996; Currie and Fox, 1997), with the general trend that N-type channels are more strongly modulated than P/Q-type channels (but see Meza and Adams, 1998). As well, the contrasts in the extent of modulation may relate to certain quantitative differences in the kinetics of $G_{\beta\gamma}$ interaction with N- and P/Q-type channels (Zhang et al., 1996). However, it is unknown whether there are fundamental qualitative differences in the modulation of N- and P/Q-type channels, and there remain substantial gaps in the comparison of G-protein modulation of these two channels, particularly as determined under uniform experimental conditions.

Here, the overall goal was to undertake in-depth analyses of the G-protein inhibition of N- and P/Q-type calcium channels, exploiting reconstitution of such modulation in HEK 293 cells transfected with recombinant channels and receptors. To articulate the specific scope of the experiments and results, we first review the "willing-reluctant" model of voltage-dependent G-protein inhibition of neuronal calcium channels (Bean, 1989; Elmslie et al., 1990), a leading mechanistic framework for rationalizing the key functional features of this form of modulation. According to this model (Fig. 1), uninhibited channels exist in a "willing" mode of gating in which depolarization induces ready opening of the channel in state O, and activated G proteins inhibit the channel by favoring occupancy of a "reluctant" mode of gating where longer and/or stronger depolarizations are required to open in state O′ (G-protein inhibited). As activation of current entails voltage-dependent movement of channels through a series of closed states (C in the willing mode, C′ in the reluctant mode) to their respective open states (O and O′), the contrasting propensities to open in the two modes reflect quantitative differences in their respective activation pathways (Jones et al., 1997). Elmslie et al. (1990) explicitly incorporated the idea that conversions between willing and reluctant modes of gating reflect binding and unbinding of activated G proteins to and from the channel. The voltage dependence of G-protein inhibition, alluded to above in relation to the tendency for depolarization to transiently relieve inhibition, is explained by the proposed state dependence of $G_{\beta\gamma}$ binding to the channel (Boland and Bean, 1993): $G_{\beta\gamma}$ is presumed to have a high affinity for channels in deep closed conformations towards the left of each mode, and a lower affinity for conformations near or in the open states (O and O′). Hence, by driving channels towards different

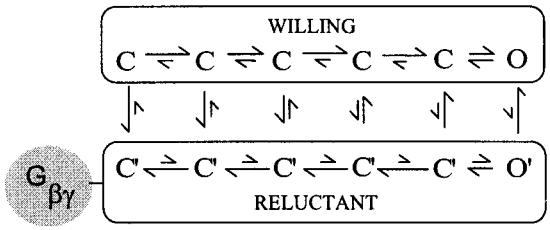

Figure 1. State diagram showing key features of the willing–reluctant model of G-protein inhibition of neuronal Ca^{2+} channels. The willing mode of gating represents the activation process of uninhibited channels, those to which $G_{\beta\gamma}$ has not bound. C, closed states; O, open state. Depolarization rapidly drives the channel rightward through voltage-dependent transitions, resulting in robust opening of the channel. $G_{\beta\gamma}$ binding causes channels to adopt a reluctant mode of gating, in which C′ are closed states and O′ is the open state. By contrast to the willing mode, depolarization of channels in the reluctant gating mode open poorly or slowly, if at all. The vertical transitions, which correspond to binding and unbinding of G proteins, are considered to be voltage independent because $G_{\beta\gamma}$ binds to cytoplasmic channel structures outside the membrane field. $G_{\beta\gamma}$ binding to the channel is state dependent in that the tendency for binding decreases as the channel occupies states towards the right, near the open state. This trend is represented diagrammatically by the relative length of transition arrows.

positions along the activation pathway, changes in voltage alter $G_{\beta\gamma}$ affinity and thereby redistribute channels between willing and reluctant modes.

Classic features of voltage-dependent inhibition are then explained in the following manner. (a) The slowing of the activation process induced by G proteins ("kinetic slowing") (Luebke and Dunlap, 1994) corresponds to depolarization driving reluctant channels towards conformations near the reluctant open state (O′), whereupon $G_{\beta\gamma}$ dissociates slowly and allows initially reluctant channels to open in the willing mode with higher open probability (Elmslie et al., 1990; Boland and Bean, 1993; Patil et al., 1996; Jones and Elmslie, 1997). In this scenario, the gradual time course of $G_{\beta\gamma}$ unbinding accounts for the slow phase of activation. (b) The relative extent of inhibition is generally diminished with increasing depolarization (Bean, 1989; Boland and Bean, 1993), possibly because either the $G_{\beta\gamma}$ dissociation described above is more complete, or reluctant channels are forced open to a greater extent. (c) The transient relief of inhibition measured during a test pulse that follows a large depolarizing prepulse ("prepulse facilitation") (Forscher and Oxford, 1985; Marchetti et al., 1986; Elmslie et al., 1990; Boland and Bean, 1993; Mintz and Bean, 1993; Hille, 1994) could occur because the prepulse brings about $G_{\beta\gamma}$ dissociation, which is only partially reversed during a short interpulse. Hence, the population of channels is still biased towards the willing mode during the ensuing test pulse, resulting in facilitation of current.

The reluctant–willing model points to a crucial dif-

ference that could exist among different channels in regard to the prevalence of reluctant openings. In some channel types, the kinetic structure of the channel might enforce a "preferential exchange" scenario (Patil et al., 1996), in which $G_{\beta\gamma}$ unbinding always predominates before appreciable opening of reluctant channels. In other channel types, a "permissive exchange" scenario may hold (Patil et al., 1996), where sufficiently strong depolarization is capable of driving reluctant channels to open appreciably in O′ before bound $G_{\beta\gamma}$ subunits have time to unbind (Elmslie et al., 1990; Boland and Bean, 1993). These two scenarios predict fundamentally different effects of G-protein inhibition on the waveform of Ca^{2+} entry during action potentials (Brody et al., 1997), with potentially important physiological consequences for the timing and efficacy of synaptic transmission (Bertram et al., 1996; Borst and Sakmann, 1998; Sabatini and Regehr, 1999).

In this study, we provide evidence for a fundamental qualitative difference in the G-protein modulation of N- versus P/Q-type calcium channels. Using whole-cell voltage-clamp techniques and novel analyses, we provide compelling arguments that reluctant openings readily occur in N-type channels at physiologically relevant voltages. By contrast, occupation of the reluctant open state appears to be rare for P/Q-type channels.

MATERIALS AND METHODS

Expression of Recombinant Channels and Receptors

Low passage number HEK 293 cells (<20 passages) were transiently transfected with 8 μg each of cDNAs encoding calcium channel α_{1A} (rat brain, rbA-1) (Stea et al., 1994) or α_{1B} (human, $\alpha_{1B\text{-}1}$) (Williams et al., 1992), rat brain β_{2a} (Perez-Reyes et al., 1992), and rat $\alpha_{2b}\delta$ subunits (Tomlinson et al., 1993), together with 2 μg cDNA encoding the m2 muscarinic receptor (Peralta et al., 1987), using the calcium phosphate precipitation method. All constructs were subcloned into cytomegalovirus expression plasmids. HEK 293 cells were maintained as previously described (Brody et al., 1997).

Electrophysiology

Whole cell currents were obtained at room temperature, 2–3 d after transfection, by standard patch clamp methods with an Axopatch 200A (Axon Instruments). Cells were continuously perfused with a bath solution containing (mM): 150 tetraethylammonium methane sulfonate (TEA-$MeSO_3$), 2 $CaCl_2$, 1 $MgCl_2$, and 10 HEPES, pH 7.4 adjusted with TEA-OH. Where noted, 50 μM carbachol was included in the superfusing medium to activate G-proteins via the transfected m2 muscarinic receptor. Internal solution contained (mM): 135 Cs-$MeSO_3$, 5 CsCl, 10 EGTA, 1 $MgCl_2$, 4 MgATP, 0.3 LiGTP, and 10 HEPES, pH 7.3 adjusted with CsOH. Pipette series resistances were typically <1 MΩ after 70–80% compensation. In protocols in which tail currents were analyzed, signals were filtered at 10 kHz (four-pole Bessel) and sampled at 20-μs intervals. In protocols in which step currents alone were analyzed, signals were filtered at 2 kHz and sampled every 40 μs. Data traces were acquired at a repetition interval of 30 s. All voltages were corrected for a liquid junction potential of −11 mV before recording. Leaks and capacitance transients were subtracted by a P/8 protocol. For displayed traces, we often subtracted a smooth curve fitted to the leak currents. Data were analyzed using custom-written MATLAB software (MathWorks). Pooled data are presented as mean ± SEM.

RESULTS

Reconstitution of Voltage-dependent G-Protein Inhibition of N- and P/Q-type Calcium Channels

Transfection of HEK 293 cells with cDNA encoding the N-type ($\alpha_{1B}/\beta_{2a}/\alpha_2\delta$) or the P/Q-type ($\alpha_{1A}/\beta_{2a}/\alpha_2$) calcium channel, along with the m2 muscarinic receptor, enabled the recording of robust Ca^{2+} currents that could be modulated by the muscarinic agonist carbachol (CCh). Application of a supramaximal dose of CCh (50 μM) resulted in the inhibition of both N- and P/Q-type Ca^{2+} currents (Figs. 2 and 3) in a manner that recapitulated classic features of voltage-dependent inhibition, as observed in neurons (Bean, 1989; Kasai, 1992) and heterologous systems expressing recombinant channels (Patil et al., 1996). First, application of CCh produced kinetic slowing of channel activation (Luebke and Dunlap, 1994), as evident from comparison of exemplar currents in the absence (−CCh) and presence (+CCh) of carbachol (Figs. 2 and 3, left). By contrast to control currents, which primarily activated according to a single rapid component, inhibited traces showed clearly distinguishable fast and slow components of activation. Such kinetic slowing resulted in the degree of inhibition being greatest when measured shortly after the start of depolarization, after appreciable activation of the fast, but not slow component. Henceforth, inhibition of test-pulse current was therefore quantified via peak current determined in the interval between 3 and 5 ms from the start of voltage steps, a parameter that conveniently approximates the amplitude of the fast-activating component. A second feature was the full reversibility of inhibition during maintained depolarization, as demonstrated by the convergence of inhibited and control traces at the end of depolarizing steps to sufficiently positive potentials. This finding implies the reconstitution of a purely voltage-dependent form of G-protein inhibition of both channel types. Convergent, voltage-independent mechanisms of G-protein inhibition are also present in certain preparations (Hille, 1992; Luebke and Dunlap, 1994); their absence in HEK 293 cells simplifies subsequent in-depth analysis of the voltage-dependent mechanism alone. Another perspective on the voltage-dependent nature of inhibition came from comparison of current–voltage relations ±CCh (Figs. 2 A and 3 A, right). Inhibition of current was largest at low or moderate depolarizations, but essentially absent at voltages greater than +40 mV (Bean, 1989; Boland and Bean, 1993). Finally, although the relief of inhibition by depolarization was transient, the relief did persist for some milliseconds after large depolarizing prepulses (Figs. 2 B and 3 B, left), in a fashion

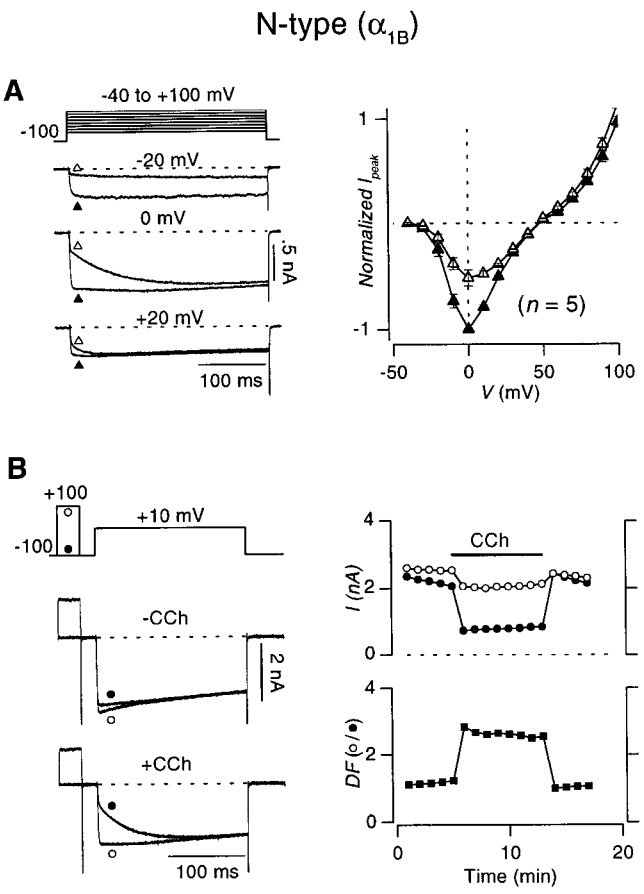

Figure 2. Carbachol-induced inhibition of recombinant N-type (α_{1B} β_{2a} $\alpha_2\delta$) channels expressed in HEK 293 cells. (A, left) Voltage protocol and whole-cell currents elicited by 300-ms depolarizations to indicated voltages in the absence (▲) or presence (△) of 50 μM carbachol. Tail currents are clipped for display clarity throughout this figure. (A, right) Plot of current (I_{peak}) vs. voltage (V) in the absence (−CCh, ▲) or presence (+CCh, △) of carbachol, averaged from the number of cells indicated in parentheses. Error bars shown where larger than symbols, here and throughout. I_{peak} values are maximal currents determined within a window extending from 3 to 5 ms after the onset of depolarization. Before averaging, values were normalized to the peak current obtained at 0 mV without CCh. (B, left) Voltage protocol and exemplar whole-cell currents elicited using 200-ms depolarizations to +10 mV, with (○) or without (●) a 30-ms prepulse to +100 mV without (upper traces) or with (lower traces) CCh. The interpulse duration was 20 ms. (B, top right) Diary plot of current traces obtained with (○) or without (●) a prepulse from the exemplar cell used on the left. (B, bottom right) Diary plot of degree of facilitation (DF, ■), the ratio of test-pulse I_{peak} with prepulse to test-pulse I_{peak} obtained without a prepulse.

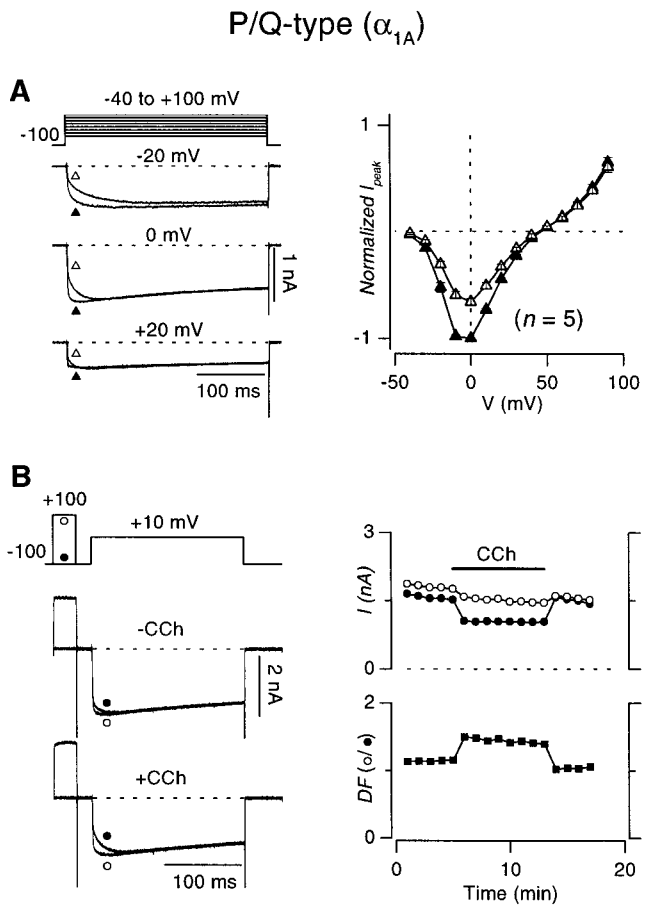

Figure 3. Carbachol-induced inhibition of recombinant P/Q-type (α_{1A} β_{2a} $\alpha_2\delta$) channels expressed in HEK 293 cells. Format identical to that in Fig. 4.

that recapitulated prepulse facilitation as observed in neurons (Grassi and Lux, 1989; Elmslie et al., 1990). Under control conditions (−CCh), the amplitude of the fast-activating component of test-pulse current was barely larger after a 30-ms prepulse to +100 mV (○) than without a prepulse (●), consistent with minimal basal activation of G proteins. However, in the presence of CCh, the prepulse produced marked facilitation of test-pulse currents (○), with fast-activating components nearly as large as observed without CCh (Figs. 2 B and 3 B, right). Interestingly, basal inhibition was completely absent upon washout of CCh (Figs. 2 B and 3 B, right) (Roche and Treistman, 1998).

Although these results suggested that G-protein inhibition of the recombinant N-type channel was broadly similar to that of the P/Q-type channel, closer examination of the exemplar data (Figs. 2 and 3) pointed to quantitative differences that might exist in the degree of inhibition and facilitation, as observed elsewhere (Mintz and Bean, 1993; Bayliss et al., 1995; Bourinet et al., 1996; Zhang et al., 1996; Currie and Fox, 1997; Roche and Treistman, 1998). Population data from a number of cells firmly established this impression. N-type currents evoked by step depolarizations to +10 mV were inhibited by 48.8 ± 1.3% (n = 13), compared with 34.5 ± 2.4% (n = 9; $P < 0.005$, one-tailed unpaired t test) for P/Q-type channels, comparable with the degree of inhibition observed in native preparations (Bean, 1989; Mintz and Bean, 1993; Currie and Fox, 1997). The stronger inhibition resulted in greater prepulse facilitation of N-type channels (2.69 ± 0.31-fold, n = 7) com-

pared with P/Q-type channels (1.50 ± 0.07-fold, $n = 6$; $P < 0.005$, one-tailed unpaired t test), as determined by the voltage protocols in Figs. 2 B and 3 B.

Tail G-V Relations Hint at Fundamental Differences in the Prevalence of "Reluctant Openings" in N- and P/Q-type Channels

Having established the overall modulatory behavior of N- and P/Q-type channels, we turned to experiments that suggested a more fundamental, qualitative difference in the prevalence of reluctant openings manifested by these channels. Tail G-V protocols usually feature relatively long (10–20 ms) voltage steps preceding tail currents. With such relatively long depolarizing steps, the reluctant–willing model predicts two mechanisms by which the tail G-V curve with CCh should be right-shifted with respect to the control curve without CCh (Bean, 1989; Mintz and Bean, 1993; Patil et al., 1996). First, strong depolarization is required for $G_{\beta\gamma}$ to unbind from reluctant channels (Fig. 4 A, pathway *a*), permitting subsequent high probability opening in the willing mode. Second, channels in the reluctant mode might exhibit reluctant openings (O′) within the same mode (Fig. 4 A, pathway *b*), but only with strong depolarization. Both mechanisms predict that greater depolarization is required to open channels that are initially in the reluctant mode, compared with that required to open initially willing channels.

If the duration of the voltage step preceding tail cur-

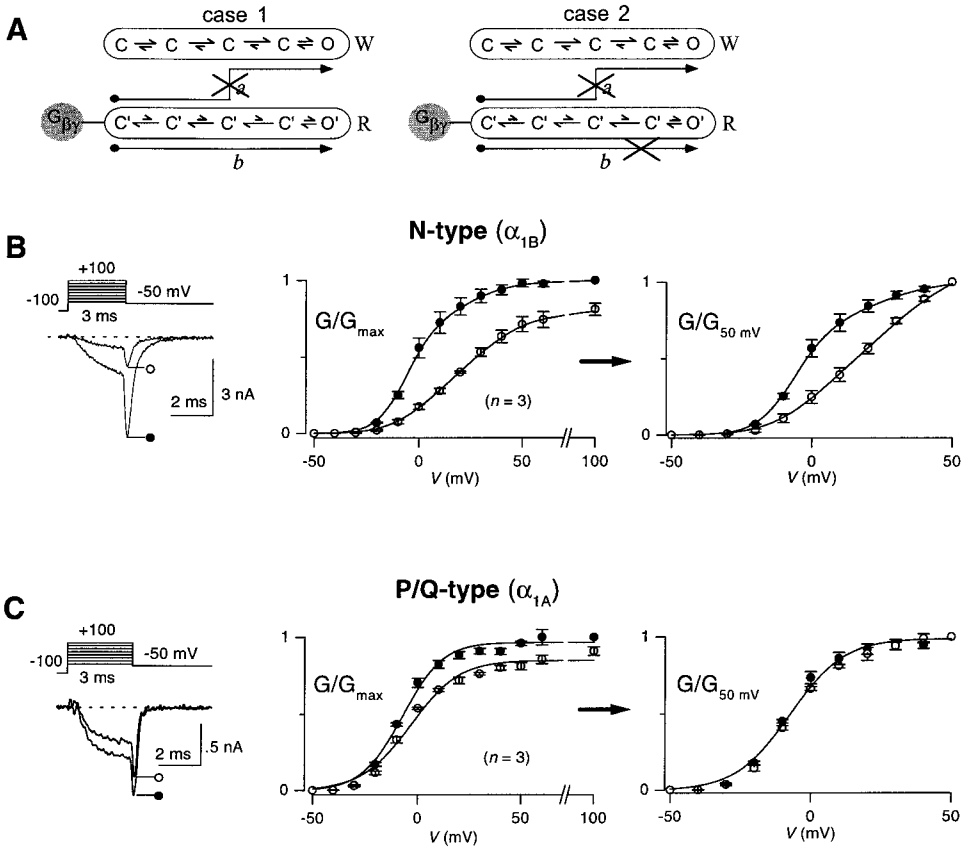

Figure 4. Tail-activation (G-V) curves for G-protein–inhibited recombinant N- and P/Q-type channels. (A) Two pathways (*a* and *b*) by which initially reluctant channels can be found open in tail currents at −50 mV, following voltage steps to different voltages. In *a*, initially reluctant channels convert to willing channels during the depolarization and are found open in the willing mode open state (O) upon repolarization that elicits tail current. In *b*, initially reluctant channels stay in the reluctant mode during the depolarization and are found in the reluctant open state (O′) in the tail current. With customary protocols featuring relatively long (10–20 ms) voltage steps, *a* is possible because the 10–20-ms depolarizing interval gives sufficient time for reluctant → willing mode conversion (Fig. 10 B). However, by using a tail-activation protocol with a 3-ms depolarizing step, the brief duration of the depolarizing step makes it unlikely that appreciable reluctant → willing mode conversion could occur, effectively prohibiting opening by *a*. In case 1, initially reluctant channels manage to populate the reluctant open state (O′) in the tail current elicited by repolarization at the end of a 3-ms depolarizing step. Appreciable opening by *b* would produce a right shift in normalized G-V curves. In case 2, initially reluctant channels cannot reach O′ by the end of a 3-ms depolarizing step. No right shift in normalized G-V curves would occur in this scenario. (B) Tail-activation curves for N-type channels, with 3-ms depolarizations. (Left) Voltage protocol and exemplar tail currents ± CCh after depolarization to 0 mV. (Middle) tail G-V curves, obtained in the presence (○) or absence (●) of CCh, averaged from the indicated number of cells. G/G_{max} values were obtained by normalizing peak tail currents with maximal tail currents after +100-mV steps, recorded without CCh. (Right) Normalized G-V curves, obtained from the same cells as used on the left. Peak tail currents obtained −CCh were normalized with the amplitude of the −CCh tail current elicited by 50-mV step depolarization. Peak tail currents obtained +CCh were normalized by the +CCh tail current after 50-mV depolarization. These ratios give rise to the plotted $G/G_{50\ mV}$ values. The right shift of the normalized G-V curve ($G/G_{50\ mV}$ vs. V) obtained +CCh (○) favors reluctant channel opening according to *b* in A. Smooth curves are dual Boltzmann functions fitted by eye. We did not interpret the Boltzmann parameters, as Boland and Bean (1993) found that such curve fitting was not precise enough for in-depth mechanistic distinctions. (C) Tail-activation curves for P/Q-type channels, with 3-ms depolarizations. Format identical to B. (Right) Absence of right shift of the normalized G-V curve ($G/G_{50\ mV}$ vs. V) obtained +CCh (○) argues against reluctant channel opening according to *b* in A.

rents is reduced to 3 ms (Fig. 4), then the reluctant–willing model predicts only one mechanism by which carbachol would right-shift the G-V curve. Given that the measured time constant for exchange between reluctant and willing modes is >10 ms for voltages up to +50 mV (see Fig. 10), relatively little depolarization-driven conversion from reluctant to willing modes should occur within 3 ms, thus minimizing the first mechanism for right-shifting G-V curves (Fig. 4 A, pathway *a*). The only remaining mechanism requires that strong depolarization be capable of forcing reluctant channels to open in O′ (Fig. 4 A, case 1, pathway *b*). If depolarization cannot induce such reluctant openings, then initially reluctant channels would not open appreciably by any pathway (Fig. 4 A, case 2). In the latter case, the overall G-V curve with CCh would be a scaled-down version of the uninhibited G-V curve, where the reduction in amplitude scales directly with the carbachol-induced decrease in the number of initially willing channels. Fig. 4 B summarizes the results of this test for reluctant openings, as applied to N-type channels. With 3-ms depolarizations preceding tail currents, the tail G-V appears right-shifted and smaller in amplitude with CCh than without (Fig. 4 B, middle). The actual test comes with normalization of the G-V curves ±CCh relative to each other (Fig. 4 B, right). To satisfy the test prerequisite that interchange between reluctant and willing modes be minimal, the curves were normalized at +50 mV, and interpretation was limited to more negative potentials. After such normalization, the normalized G-V curve with CCh displayed a prominent rightward shift in the relevant voltage range (Fig. 4 B, right), clearly contradicting the predicted outcome for no reluctant openings, and instead supporting their robust presence. In striking contrast, tail G-V curves for control and G-protein–inhibited P/Q-type channels essentially coincided after normalization at +50 mV (Fig. 4 C), suggesting the virtual absence of reluctant openings. This remarkable difference in the behavior of normalized G-V curves for N- and P/Q-type channels provided the first suggestion of a fundamental qualitative difference in the G-protein inhibition of N- versus P/Q-type channels: it appeared that inhibited N-type, but not P/Q-type channels could open in the reluctant mode.

The strength of this suggestion was critically dependent on the extent to which exchange between reluctant and willing modes was minimized by the 3-ms duration of depolarizing steps. Furthermore, the experimental design in Fig. 4 did not provide a practical approach to estimate the relative prevalence of reluctant openings at various voltages, as would be required to gauge the relevance of such openings at physiological potentials. These limitations motivated the development of a complementary strategy for determining the prevalence of reluctant openings.

"Slope-Analysis" Method for Detection of Reluctant Openings

As a starting point for developing the complementary strategy, we applied a voltage protocol similar to one initially described by Boland and Bean (1993). Fig. 5 A shows the specific paradigm, which compares the kinetics of N-type channel activation with the time evolution of prepulse facilitation, all during exposure to carbachol. Activation was gauged by the amplitude of the tail current (I_{tail}) at −30 mV, following 100-mV prepulses of increasing duration. Facilitation was gauged by the increase in the fast-activating phase of the current (I_{peak}) elicited by an ensuing test pulse to +10 mV. The time courses of the two processes are shown in Fig. 5 B, where normalized versions of these parameters, $I_{tail,norm}$ (●) and $I_{peak,norm}$ (○), reflect activation and facilitation, respectively. The $I_{tail,norm}$ curve indicated a roughly biexponential time course of activation (smooth curve), the slow phase of which is a familiar feature of kinetic slowing. The time course of facilitation could be represented by a constant offset plus a single exponential with $\tau = 5.5$ ms. If channels in the reluctant mode cannot open, even with the 100-mV depolarization during the prepulse, then the slow phase of activation and the time course of facilitation (Fig. 5 B) would be expected to coincide precisely in amplitude and time course, because both plots reflect unbinding of G proteins, and only willing channels can open. As shown in Fig. 5 B, however, the plots for these two processes are clearly disjoint (Boland and Bean, 1993), which argues for the occurrence of reluctant openings in N-type channels during prepulse depolarization to +100 mV.

Quantitative conceptualization of the experiment in Fig. 5 enabled us to generalize the approach, leading to a slope analysis method for detecting reluctant openings at different voltages. To articulate this novel method, we first developed equations that provide a first-order description of the processes of facilitation and activation. Fig. 6, A–C, shows fits of these equations to the N-type channel data in Fig. 5, using a format that aids intuitive understanding of the functional forms. The normalized time course of facilitation ($I_{peak,norm}$) is shown in Fig. 6 A, and can be described as:

$$I_{peak,\,norm} = A_{initial,\,peak} + A_{slow,\,peak}(1 - e^{-D/\tau}), \qquad (1)$$

where $A_{initial,peak}$ and $A_{slow,peak}$ are the magnitudes of the initial constant offset and slow-exponential component of the curve, D is the prepulse duration, and τ is presumably the time constant for conversion of initially reluctant channels into the willing mode. If we assume that the modest test potential (+10 mV) used to elicit I_{peak} does not evoke appreciable reluctant openings, it follows that the amplitude of the initial offset would scale directly with the fraction of initially willing channels at the holding potential (F_W), normalized by the

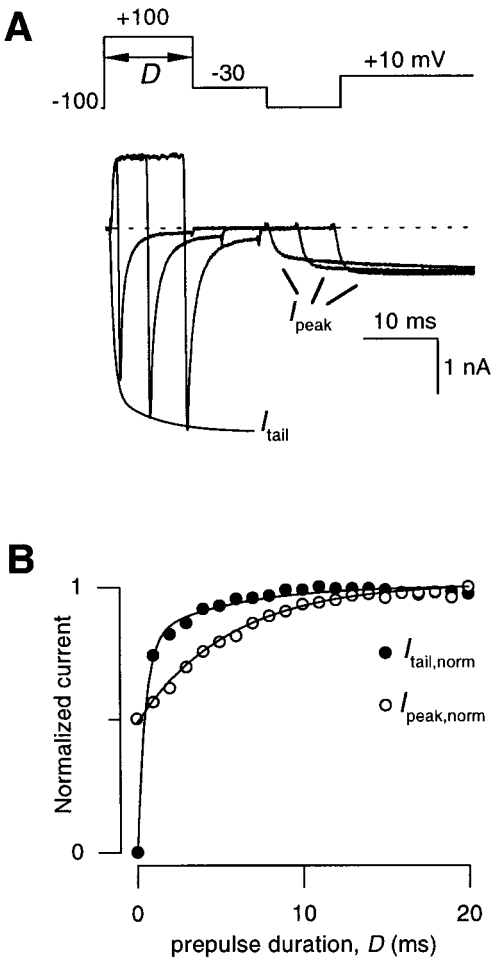

Figure 5. Time courses of facilitation and activation in recombinant N-type channels. (A) Variable-duration prepulse protocol used to simultaneously determine the time courses of activation (I_{tail}) and facilitation (I_{peak}) of N-type currents obtained +CCh. Activation was followed by measuring amplitudes of tail currents at −30 mV (I_{tail}) following prepulses of varying duration (D) to +100 mV, while facilitation was followed by measuring the peak current obtained during an ensuing test pulse to +10 mV (I_{peak}). I_{peak} is peak current as determined within a window extending from 3 to 5 ms from the onset of depolarization to +10 mV. Displayed traces were obtained with prepulse durations of 1, 6, and 11 ms. The smooth curve describing the "envelope" of I_{tail} is a biexponential fit to the entire ensemble of tail currents. (B) Plot of the time courses of activation ($I_{tail,norm}$) and facilitation ($I_{peak,norm}$) taken from the exemplar cells in A. Currents were normalized to amplitudes of tail and peak currents obtained after a 20-ms prepulse, yielding $I_{tail,norm}$ and $I_{peak,norm}$), respectively. Smooth curve through normalized tail current data is a least-squares fit by a biexponential function:

$$I_{tail,\,norm} = I_{tail}/I_{tail,\,max} = A_{fast,\,tail}(1-e^{-D/\tau_{fast,\,tail}}) + A_{slow,\,tail}(1-e^{-D/\tau}),$$

with the fractional amplitude of the fast component $A_{fast,tail} = 0.8$, $A_{slow,tail} = 1 - A_{fast,tail} = 0.2$, $\tau_{fast,tail} = 0.49$ ms, and $\tau = 5.5$ ms. Smooth curve through normalized peak current data is a least-squares fit by a single exponential function (Eq. 4), with $A_{initial,peak} = 0.48$, $A_{slow,peak} = 1 - A_{initial,peak} = 0.52$, and the same τ as above.

fraction of willing channels that would be observed with prolonged depolarization at the prepulse voltage V_{pre}. The normalization factor would then be $F_W + [F_R - F_{Rmin}(V_{pre})]$, where the term in parentheses is the increase in the fraction of willing channels over the course of maintained depolarization to V_{pre}, F_R is the fraction of initially reluctant channels at the holding potential, and $F_{Rmin}(V_{pre})$ is the fraction of channels that would remain in the reluctant mode during maintained depolarization to V_{pre}. As such, F_W and F_R depend on the magnitude of the steady state inhibition at the holding potential (always −100 mV), and F_{Rmin} depends on the steady state inhibition at various step potentials. The initial offset amplitude is therefore:

$$A_{initial,\,peak} = \frac{F_W \cdot P_o(V_{test})}{F_W \cdot P_o(V_{test}) + [F_R - F_{Rmin}(V_{pre})] \cdot P_o(V_{test})} = \frac{F_W}{F_W + F_R - F_{Rmin}(V_{pre})}, \quad (2)$$

where $P_o(V_{test})$ is the steady state open probability of willing channels at V_{test}. Because the amplitudes of the initial offset and slow-exponential component sum to unity, the slow-exponential amplitude must be $1 - A_{initial,peak}$, which is:

$$A_{slow,\,peak} = \frac{F_R - F_{Rmin}(V_{pre})}{F_W + F_R - F_{Rmin}(V_{pre})}. \quad (3)$$

The contributions of these two amplitudes are represented graphically in Fig. 6 A.

Similarly, after the fast phase of activation has occurred, the normalized time course of channel activation can be represented as (Fig. 6 B):

$$I_{tail,\,norm} = A_{fast,\,tail} + A_{slow,\,tail}(1-e^{-D/\tau}), \quad (4)$$

where $A_{fast,tail}$ is the amplitude of the fast-activating component and $A_{slow,tail}$ is the amplitude of the slow-activating component. During strong depolarization, $A_{fast,tail}$ may have contributions from the opening of both willing and reluctant channels, as specified by:

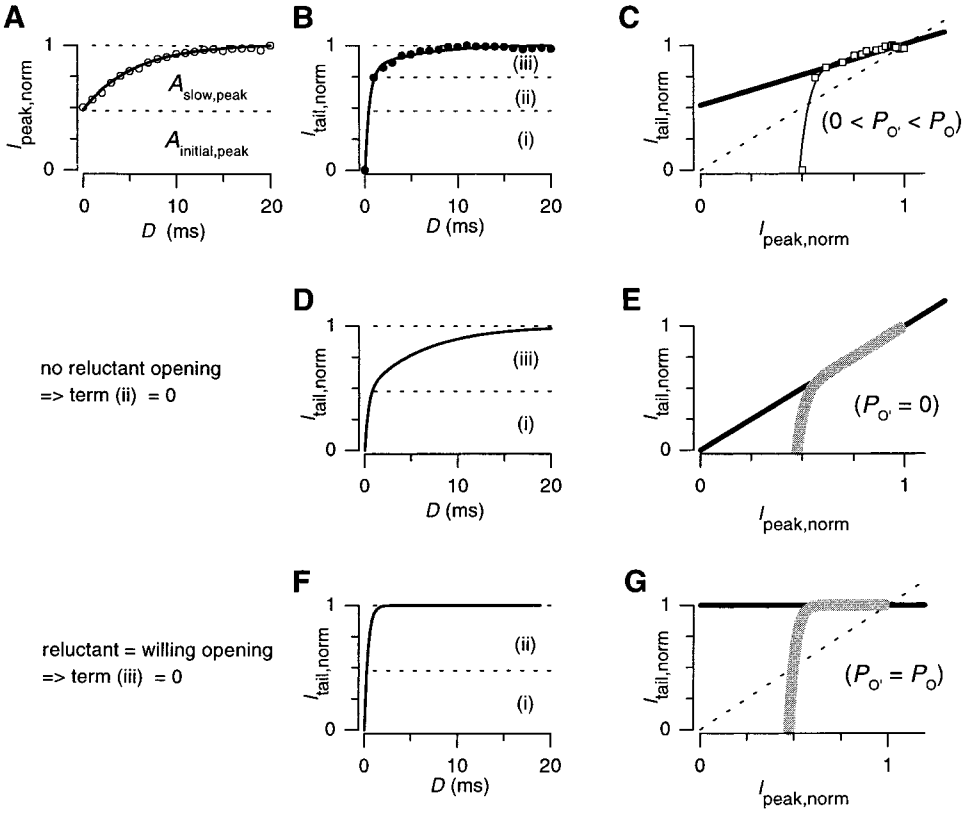

Figure 6. Slope-analysis method for determination of reluctant openings. (A and B) Reproduction of data and least-squares fits for the normalized time courses of facilitation ($I_{peak,norm}$) and activation ($I_{tail,norm}$) from Fig. 5 B. (C) Curvilinear relationship between $I_{peak,norm}$ and $I_{tail,norm}$ (□), formed from data in A and B. Solid line through the linear portion of the curve was drawn from the equation: $I_{tail,norm} = 0.49 \times I_{peak,norm} + 0.51$. The dashed line is the line of identity. (D and E) Simulations of anticipated activation time course (D) and $I_{tail,norm} - I_{peak,norm}$ relation (E, gray curve), under the condition that no reluctant openings occur (i.e., when $P_{o'} = 0$). Solid line through linear portion of simulated $I_{tail,norm} - I_{peak,norm}$ curve (E) lies on the line of identity. (F and G) Simulations of anticipated activation time course (F) and $I_{tail,norm} - I_{peak,norm}$ relation (G, gray curve), under the condition that reluctant channels open just as well as willing channels (i.e., when $P_{o'} = P_o$). The dashed line is the line of identity.

$$A_{fast,\,tail} = \underbrace{\frac{F_W \cdot P_o(V_{pre})}{S}}_{i} + \underbrace{\frac{F_R \cdot P_{o'}(V_{pre})}{S}}_{ii}$$

$$S = F_W \cdot P_o(V_{pre}) + F_R \cdot P_{o'}(V_{pre}) + [F_R - F_{Rmin}(V_{pre})] \cdot [P_o(V_{pre}) - P_{o'}(V_{pre})], \quad (5)$$

where $P_o(V_{pre})$ is the steady state open probability of willing channels at V_{pre}, and $P_{o'}(V_{pre})$ is the steady state open probability of reluctant channels at V_{pre}. *i* and *ii* reflect the respective normalized contributions of initially willing and reluctant channels to overall opening in the fast-activating phase, and the magnitudes of these two terms are represented graphically in Fig. 6 B. The scaling factor S in the denominator reflects the overall open probability that would be expected during maintained depolarization to V_{pre}. S therefore includes not only two terms corresponding to the contributions of initially willing and reluctant channels $[F_W P_o(V_{pre}) + F_R P_{o'}(V_{pre})]$, but an additional term representing the increased open probability brought about by that fraction of channels that converts from reluctant to willing modes $\{[F_R - F_{Rmin}(V_{pre})] \times [P_o(V_{pre}) - P_{o'}(V_{pre})]\}$. The slow component of $I_{tail,norm}$ reflects the same increase in open probability brought about by that fraction of channels that converts from reluctant to willing modes.

The amplitude of the slow component, represented graphically in Fig. 6 B, *iii*, is easily calculated from $1 - A_{fast,tail}$ as:

$$A_{slow,\,tail} = [F_R - F_{Rmin}(V_{pre})] \cdot [P_o(V_{pre}) - P_{o'}(V_{pre})] / \{F_W \cdot P_o(V_{pre}) + F_R \cdot P_{o'}(V_{pre}) + [F_R - F_{Rmin}(V_{pre})] \cdot [P_o(V_{pre}) - P_{o'}(V_{pre})]\}. \quad (6)$$

The basis of the slope analysis method for determining the occurrence of reluctant openings came from the realization that a linear relationship exists between activation ($I_{tail,norm}$) and facilitation ($I_{peak,norm}$). This can be shown by combining Eqs. 1 and 4, yielding:

$$I_{tail,\,norm} = \left(\frac{A_{slow,\,tail}}{A_{slow,\,peak}}\right) \cdot I_{peak,\,norm} + \left[A_{fast,\,tail} - \left(\frac{A_{slow,\,tail}}{A_{slow,\,peak}}\right) \cdot A_{initial,\,peak}\right]. \quad (7)$$

It was gratifying that the plot of experimentally determined $I_{tail,norm}$ as a function of $I_{peak,norm}$ actually formed a straight line (Fig. 6 C), after the anticipated initial deviation during the fast-activating phase of $I_{tail,norm}$ (which is not modeled in Eq. 1).

The slope of the linear phase of the curve ($A_{slow,tail}$ /

$A_{slow,peak}$) provides the crucial information regarding the prevalence of reluctant openings at V_{pre}. This can be demonstrated by considering what happens to the slope in two polar instances, as simulated in Fig. 6, D–G. In either instance, the time course of facilitation, as gauged by the plot of $I_{peak,norm}$ versus prepulse duration (D), will not change from that plotted in Fig. 6 A, because the experimental paradigm is designed to selectively detect willing openings. However, the kinetics of activation, as represented in plots of $I_{tail,norm}$ versus prepulse duration (D), will change dramatically depending on the prevalence of reluctant openings in the prepulse. First, in the case where reluctant openings fail to occur (i.e., when $P_{o'} = 0$) (Fig. 6, D and E), term *ii* in the plot of normalized activation vanishes (Fig. 6 D, and Eq. 5), so that the kinetics of activation at V_{pre} (Fig. 6 D) becomes essentially identical to that for facilitation (Fig. 6 A). Hence, in the absence of reluctant openings, the linear phase in the plot of $I_{tail,norm}$ versus $I_{peak,norm}$ will fall on the line of identity, with a slope of unity (Fig. 6 E). This outcome can be verified explicitly by inspection of Eqs. 3 and 6, which reveals that if $P_{o'} = 0$ (Eq. 8):

$$A_{slow,\,tail} = A_{slow,\,peak} = \frac{F_R - F_{Rmin}(V_{pre})}{F_W + F_R - F_{Rmin}(V_{pre})}, \quad (8)$$

so that the slope of the plot of $I_{tail,norm}$ versus $I_{peak,norm}$ becomes unity. Furthermore, inspection of Eqs. 2 and 5 reveals that when $P_{o'} = 0$:

$$A_{initial,\,peak} = A_{fast,\,tail} = \frac{F_W}{F_W + F_R - F_{Rmin}(V_{pre})}, \quad (9)$$

such that the y intercept term in Eq. 7 now vanishes. At the other extreme, if reluctant channels open just as well as willing ones (i.e., if $P_{o'} = P_o$) (Fig. 6, F and G), then $A_{slow,tail} = 0$ (Eq. 6), so that term *iii* in Fig. 6 F vanishes. In this circumstance, the linear phase of the plot of $I_{tail,norm}$ versus $I_{peak,norm}$ will be a flat line, with a value of unity and a slope of zero (Fig. 6 G).

Overall, the key insight from these equations is this: the presence of reluctant openings, where $0 < P_{o'} < P_o$, will result in slope values between 0 and 1, with lower slope values corresponding to greater occurrence of reluctant openings. The slope analysis for the actual N-type channel data in Fig. 6 C yields a slope of 0.49, indicating substantial occurrence of reluctant openings. In fact, the slope can be converted into an even more direct measure of the relative prevalence of reluctant openings, under the condition that the steady state fraction of reluctant channels $F_{Rmin}(V_{pre}) = 0$. In this case, Eqs. 3, 6, and 9 can be simplified to:

$$\frac{P_{o'}(V_{pre})}{P_o(V_{pre})} = 1 - slope. \quad (10)$$

This remarkable result should hold for voltages ≥10 mV, where the convergence of inhibited and uninhibited traces by the end of 300-ms pulses (Figs. 2 and 3) indicates that $F_{Rmin} \sim 0$. Application of this relation to the slope analysis of actual N-type channel data (Fig. 6 C) yields a relative open probability for reluctant channels of $P_{o'}/P_o = 1 - 0.49 = 0.51$ at +100 mV. Slope analysis may be applied to experiments with different prepulse voltages, enabling us to determine the propensity for reluctant channels to open at a variety of voltages.

Voltage Dependence of Reluctant Openings in N- and P/Q-type Channels

Fig. 7 summarizes the application of slope analysis to determine the occurrence and voltage dependence of reluctant openings in G-protein–inhibited N-type channels. Each of three rows corresponds to a different prepulse voltage (+50 mV in Fig. 7, A–C; +100 mV in D–F; and +150 mV in G–I). In all three instances, the occurrence of reluctant openings could be qualitatively inferred from the clear deviation of $I_{tail,norm} - I_{peak,norm}$ relations from the line of identity (Fig. 7, C, F, and I), with slope values of 0.7 (+50 mV, ○), 0.48 (+100 mV, △) and 0.32 (+150 mV, □). The population data shown below in Fig. 9 A (○) entirely confirmed these findings, with increasing voltages producing progressively more reluctant openings, and the relative open probability of reluctant channels reaching >50% at saturating depolarization. Interestingly, reluctant openings appeared to be appreciable at voltages as low as +25 mV. This would place them in a range where they could potentially contribute to physiological Ca^{2+} influx, as neuronal action potentials reach potentials as high as 30–35 mV (Borst et al., 1995).

In sharp contrast, slope analysis of P/Q-type channels revealed an entirely different picture. Fig. 8 summarizes the results, using a format identical to that applied to N-type channels (Fig. 7). The absence of reluctant openings can be qualitatively appreciated from the almost complete concurrence of slow activation and facilitation at the various prepulse voltages (Fig. 8, B, E, and H), as well as from $I_{tail,norm} - I_{peak,norm}$ relations that closely hugged the line of identity (C, F, and I). Data collected over a range of prepulse voltages in multiple cells confirmed the virtual absence of reluctant openings in P/Q-type channels (Fig. 9 A, ■). No reluctant openings could be detected at voltages up to +50 mV, and only a hint of their existence starts to appear at voltages of +100 mV or greater. Thus, in contrast to N-type channels, reluctant P/Q-type channels seem unlikely to contribute to Ca^{2+} influx during physiological action potentials.

It has been noted previously (Elmslie et al., 1990; Boland and Bean, 1993) that in G-protein–inhibited N-type channels, tail currents recorded after a brief (1–2 ms) large depolarizing prepulse deactivate faster than those recorded after a longer duration prepulse (dur-

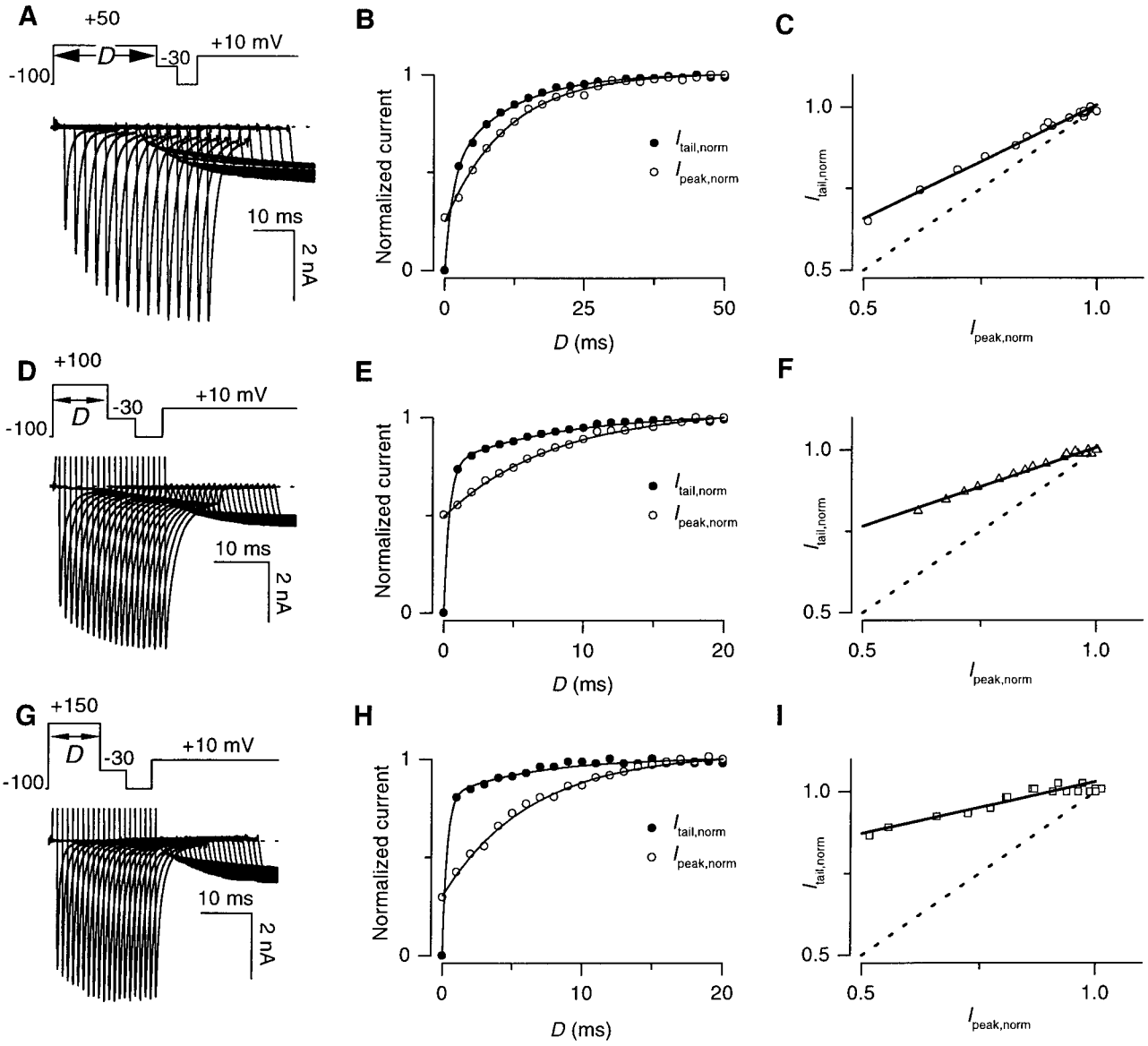

Figure 7. Reluctant openings in N-type channels detected over a range of voltages by slope analysis. (A) Variable-duration prepulse protocol and exemplar currents, analogous to those shown in Fig. 5 A. Here, however, the prepulse potential was +50 mV. Tail currents were elicited at −30 mV after prepulses of various duration (0–50 ms in 2.5-ms increments). Only the first 16 traces are shown. Peak currents were measured during an ensuing test pulse to +10 mV after an interpulse duration of 10 ms. (B) Plots of the normalized time courses of activation ($I_{tail,norm}$) and facilitation ($I_{peak,norm}$), taken from the same exemplar cell as in A. Format identical to Fig. 5 B, with parameters for least-squares fits as follows. For $I_{tail,norm}$: $A_{fast,tail} = 0.50$, $A_{slow,tail} = 1 - A_{fast,tail} = 0.50$, $\tau_{fast,tail} = 1.37$ ms, and $\tau = 11.15$ ms. For $I_{peak,norm}$: $A_{initial,peak} = 0.24$, $A_{slow,peak} = 1 - A_{initial,peak} = 0.76$, and the same τ as above. (C) Linear phase of $I_{tail,norm} - I_{peak,norm}$ relationship, drawn from exemplar data in B. The fitted solid line is $I_{tail,norm} = 0.31 \times I_{peak,norm} + 0.70$. Dashed line is the line of identity. (D–F) Slope analysis performed with prepulse voltage of +100 mV, following analogous format to *A–C*. The prepulse duration interval in D was increased in 1-ms increments. Parameter values for least-square fits in E were as follows. For $I_{tail,norm}$: $A_{fast,tail} = 0.74$, $A_{slow,tail} = 1 - A_{fast,tail} = 0.26$, $\tau_{fast,tail} = 0.39$ ms, and $\tau = 7.94$ ms. For $I_{peak,norm}$: $A_{initial,peak} = 0.48$, $A_{slow,peak} = 1 - A_{initial,peak} = 0.52$, and τ is the same as above. Fitted line in I was $I_{tail,norm} = 0.48 \times I_{peak,norm} + 0.52$. Outward currents in exemplar traces have been clipped. (G–I) Slope analysis performed with prepulse voltage of +150 mV. Format identical to that in D–F. Parameter values for least-square fits in H were as follows. For $I_{tail,norm}$: $A_{fast,tail} = 0.80$, $A_{slow,tail} = 1 - A_{fast,tail} = 0.20$, $\tau_{fast,tail} = 0.31$ ms, and $\tau = 6.29$ ms. For $I_{peak,norm}$: $A_{initial,peak} = 0.3$, $A_{slow,peak} = 1 - A_{initial,peak} = 0.7$, and τ is the same as above. Fitted line in I was $I_{tail,norm} = 0.32 \times I_{peak,norm} + 0.71$. (B, E, and H) Maximal currents used for normalization of I_{tail} and I_{peak} were obtained with prepulse durations of 50, 20, and 20 ms at prepulse voltages of +50, +100, and +150 mV, respectively. (A–I) Data from three different exemplar cells, corresponding to A–C, D–F, and G–I.

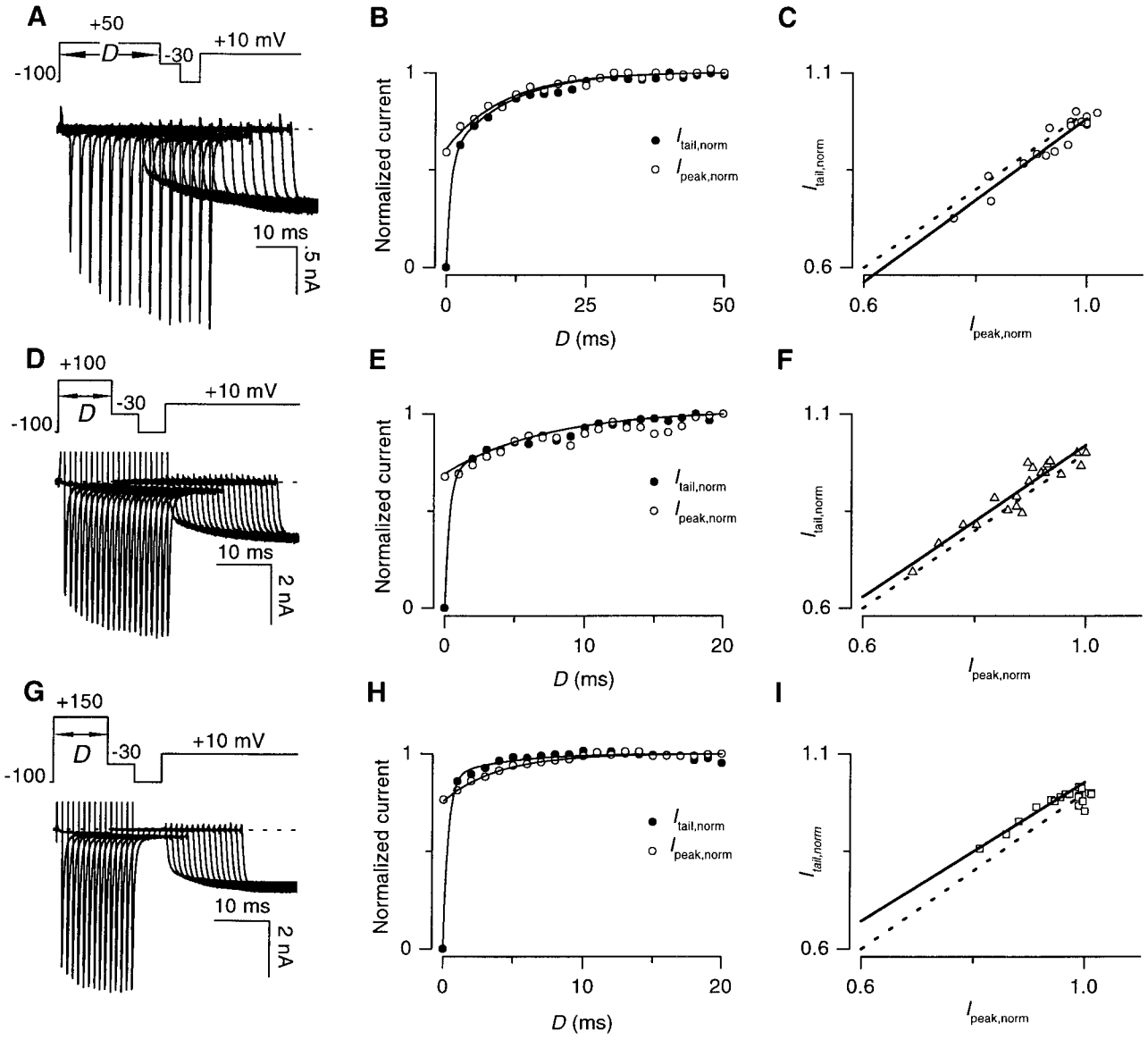

Figure 8. Virtual absence of reluctant openings in P/Q-type channels, as examined over a wide range of voltages by slope analysis. Format analogous to that in Fig. 7. (B, E, and H) Fitted exponential functions, defined in Fig. 5 B, legend, had parameters as follows. With the +50-mV prepulse in B, the $I_{tail,norm}$ parameters were: $A_{fast,tail} = 0.56$, $A_{slow,tail} = 1 - A_{fast,tail} = 0.44$, $\tau_{fast,tail} = 0.76$ ms, and $\tau = 10.5$ ms. The corresponding $I_{peak,norm}$ parameters were: $A_{initial,peak} = 0.61$, $A_{slow,peak} = 1 - A_{initial,peak} = 0.39$, and τ as above. With the +100-mV prepulse in E, the $I_{tail,norm}$ parameters were: $A_{fast,tail} = 0.68$, $A_{slow,tail} = 1 - A_{fast,tail} = 0.32$, $\tau_{fast,tail} = 0.32$ ms, and $\tau = 7.2$ ms. The corresponding $I_{peak,norm}$ parameters were: $A_{initial,peak} = 0.69$, $A_{slow,peak} = 1 - A_{initial,peak} = 0.31$, and τ as above. With the +150-mV prepulse in H, the $I_{tail,norm}$ parameters were: $A_{fast,tail} = 0.87$, $A_{slow,tail} = 1 - A_{fast,tail} = 0.13$, $\tau_{fast,tail} = 0.34$ ms, and $\tau = 3.9$ ms. The corresponding $I_{peak,norm}$ parameters were: $A_{initial,peak} = 0.76$, $A_{slow,peak} = 1 - A_{initial,peak} = 0.24$, and τ as above. (C, F, and I) Fitted linear functions were as follows. With the +50-mV prepulse in C, the line was $I_{tail,norm} = 1.04 \times I_{peak,norm} - 0.06$. With the +100-mV prepulse in F, the line was $I_{tail,norm} = 0.98 \times I_{peak,norm} + 0.04$. With the +150-mV prepulse in I, the line was $I_{tail,norm} = 0.89 \times I_{peak,norm} + 0.14$. (A–I) Data from three different exemplar cells, corresponding to A–C, D–F, and G–I.

ing which appreciable facilitation occurs). This result has been interpreted as evidence that G-protein–inhibited N-type channels could open to a reluctant open state. As a final check on the suggestion that reluctant openings occur readily in N-type, but not P/Q-type channels, we compared the kinetics of tail currents measured at −30 mV after prepulses of 1- or 20-ms duration to +100 mV, all during G-protein inhibition. In agreement with these previous studies, tail currents of inhibited N-type channels recorded after a 20-ms prepulse depolarization, deactivated at a much slower rate compared with tail currents measured after a 1-ms prepulse (Fig. 9 B, left). We further quantified the change in shape by measuring the difference in tail current width at half-maximal amplitude, which increased by 0.73 ± 0.13 ms ($n = 3$; $P < 0.05$, two-tailed paired t

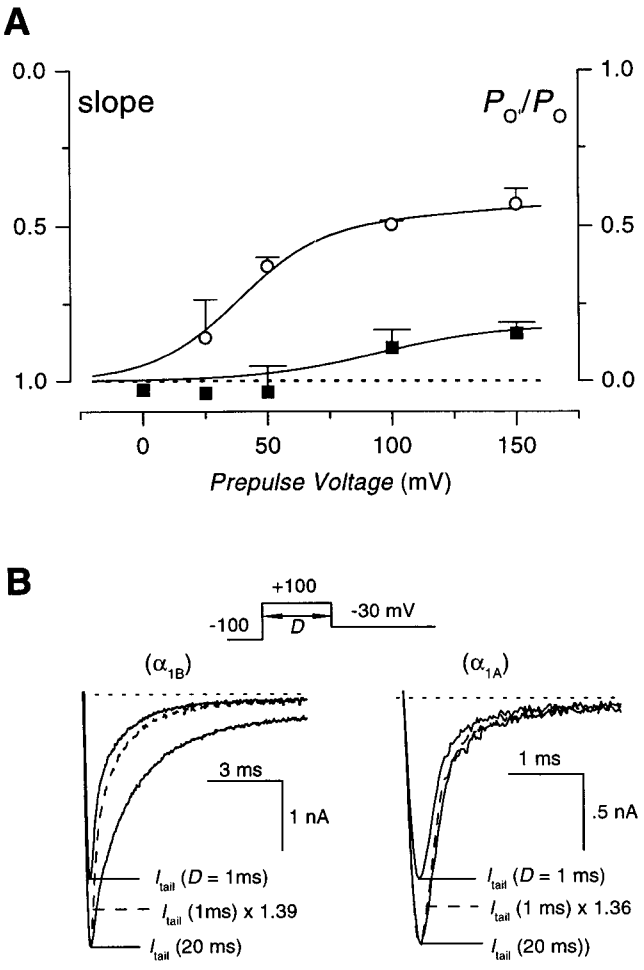

Figure 9. (A) Voltage dependence of reluctant openings in N- and P/Q-type channels. Slope values, obtained as illustrated in Figs. 7 and 8, were averaged from multiple cells. Data for G-protein–inhibited N-type (○) and P/Q-type (■) channels are plotted. Smooth curves through data points were fitted by eye. Each symbol represents the average of $n = 2$–5 cells. The y axis on the right corresponds to the relative open probability of reluctant channels ($P_{o'}/P_o$), formulated according to Eq. 10. These data indicate that N-type channels exhibit reluctant openings, with the propensity for such openings increasing with depolarization. P/Q-type channels show virtually no reluctant openings, although there is a hint of such openings at extreme depolarizations. (B) Effect of G-protein inhibition on tail current deactivation kinetics. (Top) Voltage protocol. Tail currents were recorded at −30 mV after prepulses of either 1- or 20-ms duration to +100 mV. (Bottom) Tail currents from G-protein–inhibited N-type (left) or P/Q-type (right) channels after prepulses of indicated durations. Traces shown represent averages from three cells. To permit direct visual comparison of tail-current deactivation kinetics, records obtained after a 1-ms prepulse have been scaled up (dashed line traces) to match the peak tail current amplitudes recorded after a 20-ms prepulse.

test). As a control, tail currents recorded from unmodified N channels (2 mM GDPβS included in patch pipette) displayed no appreciable lengthening, with a half-width difference of 0.11 ± 0.10 ms ($n = 3$; N.S., $P >$ 0.3, two-tailed paired t test). By contrast to inhibited N channels, tail currents from G-protein–modified P/Q channels deactivated at similar rates, irrespective of whether they were recorded after prepulse durations of 1 or 20 ms (Fig. 9 B, right; half-width difference of 0.04 ± 0.02 ms, $n = 3$; NS, $P > 0.1$, two-tailed paired t test). Thus, these tail kinetics data are consistent with the idea of a differential occurrence of reluctant openings in N- and P/Q-type channels, and therefore provide an important verification of the slope analysis method.

We considered two potential sources of artifacts that could potentially confound the interpretation of the data obtained using slope analysis. First, the faster deactivation of P/Q channels compared with N channels could induce an error if the voltage clamp was not fast enough to resolve the true peak amplitude of the P/Q-channel tail current. We addressed this issue by applying slope analysis to N-channel tail currents recorded at a more hyperpolarized voltage (−50 mV), where the N-channel deactivation rate is similar to P/Q-channel deactivation at −30 mV (data not shown). The slope values obtained from this analysis were identical to those obtained with tail currents recorded at −30 mV, thereby ruling out this potential source of error. Second, the smaller degree of inhibition of P/Q channels raised the possibility that the slope analysis method might not be sensitive enough to detect reluctant openings in P/Q channels, even if they did exist. This possibility is excluded because there are individual cases in which N channels are inhibited to a similar degree as P/Q channels, and slope analysis applied to these individual examples (not shown) resulted in slope values that did not deviate from the average values shown in Fig. 9 A.

Kinetics of $G_{\beta\gamma}$ Interaction with N-and P/Q-type Channels

What could be the molecular mechanism underlying this difference in reluctant openings between N- and P/Q-type channels? One hypothesis is that $G_{\beta\gamma}$ dissociates more quickly from P/Q- than from N-type channels (as opposed to actual differences in the activation pathways). In this case, P/Q-type channels might be capable of expressing reluctant openings if $G_{\beta\gamma}$ stayed bound long enough for such openings to occur. Since the processes of kinetic slowing and prepulse facilitation are believed to reflect unbinding of $G_{\beta\gamma}$, we investigated this possibility by comparing the time constants of slow activation (for voltages up to +30 mV) or facilitation (for voltages +50 mV or greater) between inhibited N- and P/Q-type channels (Fig. 10). Time constants for slow activation were obtained from simultaneous fits of inhibited and uninhibited traces (Fig. 10 A) as described in the legend. As there is little steady state inhibition at voltages ≥10 mV (Figs. 2 and 3), time constants are presumably equivalent to $G_{\beta\gamma}$ dissociation rates over this range of potentials. As postulated, the profile of time constants was strikingly differ-

ent between the two channel types. For the N-type channel, the time constant was comparatively slow and markedly voltage dependent, dropping precipitously from a value of 125 ± 3.9 ms at −10 mV, to a value of 7.5 ± 1.0 ms at +100 mV (Fig. 10 B). For potentials ≤20 mV, time constants for P/Q-type channels were considerably faster (15.9 ± 2.9 ms at −10 mV) and less voltage dependent than for N-type channels. Contrary to expectations of the simple hypothesis, however, time constants for the two channels converged and were virtually identical at potentials +30 mV or greater (Fig. 10 B), with a P/Q-type channel time constant of 6.1 ± 0.6 ms at + 100 mV. This convergence of time constants discounts differences in the kinetics of $G_{\beta\gamma}$ interaction with channels as a possible explanation for the differential occurrence of reluctant openings, since it is precisely at these voltages (+30 mV or greater) that reluctant openings are preferentially detected in N-type channels by the slope analysis method. Hence, under the assumption that slow activation and prepulse facilitation reflect $G_{\beta\gamma}$ unbinding from the channel, the differential occurrence of reluctant openings is likely to reflect a genuine difference in the reluctant mode activation pathways of the two channel types (Fig. 10 C), rather than differences in $G_{\beta\gamma}$ dissociation rates.

DISCUSSION

We have performed an in-depth comparison of the G-protein modulation of N- and P/Q-type calcium channels, here reconstituted in HEK 293 cells transfected with recombinant channels and receptors. As previously demonstrated for recombinant N-type channels expressed in this system (Patil et al., 1996), recombinant P/Q-type channels were also subject to a purely voltage-dependent form of G-protein modulation upon activation of transfected m2 muscarinic receptors. Overall, modulation was broadly similar for the two channel types, though N-type channels were inhibited to a greater extent, and exhibited larger prepulse facili-

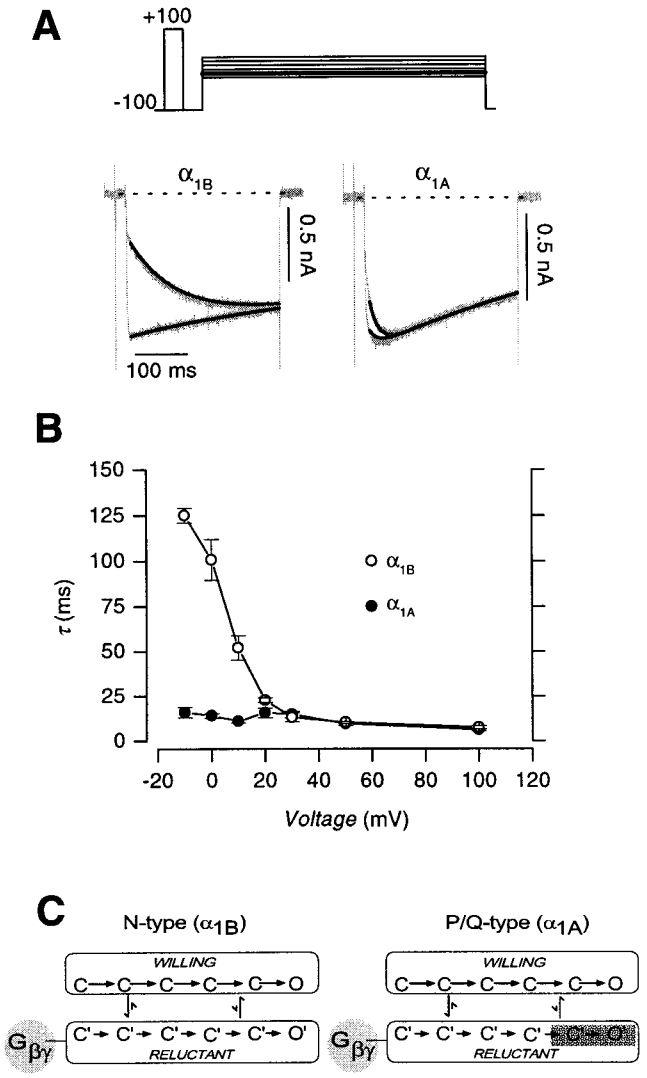

Figure 10. Comparison of N- and P/Q-type channels, in regard to the voltage dependence of time constants for facilitation and the slow phase of activation. (A, top) Voltage protocol. 300-ms test pulses to a family of voltages (ranging from −10 to +30 mV in 10-mV increments) were alternately preceded by a 20-ms prepulse to +100 mV. The interpulse duration lasted 20 ms. (A, bottom) Carbachol-inhibited N-type (α_{1B}) and P/Q-type (α_{1A}) currents (gray traces) elicited by a test pulse to 0 mV, with (larger) or without (smaller) a depolarizing prepulse. Tail and outward currents clipped for display clarity throughout this figure. Solid lines through the currents were achieved by simultaneous least-squares fits of inhibited ($I_{-\text{prepulse}}$) or uninhibited ($I_{+\text{prepulse}}$) traces using the following two equations:

$$I_{-\text{prepulse}} = [W_0 + (W_\infty - W_0)(1 - e^{-t/\tau})]e^{-t/\tau_{\text{inact.}}}$$

and

$$I_{+\text{prepulse}} = [W_\infty + (I_0 - W_\infty)(1 - e^{-t/\tau})]e^{-t/\tau_{\text{inact.}}}.$$

Parameter values for the fits to the N-type currents were: W_0 = −339.2 pA, W_∞ = −933.1 pA, I_0 = −976.1 pA, τ = 102.0 ms, $\tau_{\text{inact.}}$ = 1,666.5 ms. Parameters for fits to the P/Q-type currents were: W_0 = −609.3 pA, W_∞ = −876.9 pA, I_0 = −778.1 pA, τ = 16.9 ms, $\tau_{\text{inact.}}$ = 643.5 ms. (B) Voltage-dependent profiles of the rate of unbinding of G-protein (τ_{slow}) from inhibited N-type (○) and P/Q-type (●) channels. τ values for voltages up to +30 mV were obtained from fits to current traces as in A. τ values at +50 and +100 mV are the time course of facilitation, using voltage protocols as in Fig. 5 B. Each point averaged from n = 3–4 cells. (C) Differing kinetic models corresponding to N- and P/Q-type channels. The similarity of time constants for facilitation of N- and P/Q-type channels at voltages ≥25 mV suggests a qualitative difference in the kinetic mechanisms for reluctant gating in N versus P/Q channels. While the open state in the reluctant mode of P/Q-type channels is virtually forbidden, it can be appreciably populated in N-type channels.

tation than P/Q-type channels. The key new findings were revealed by a modified tail G-V experiment and a novel slope-analysis method, both of which indicated a more fundamental qualitative difference in the G-protein modulation of these channels. Whereas N-type channels could open in the reluctant mode of gating at physiologically relevant voltages, P/Q-type channels gave no clear indication of such reluctant openings, particularly in the physiological range of potentials ≤50 mV. In accord with previous terminology (Patil et al., 1996), our results suggest a permissive exchange model for G-protein inhibition of N-type channels, and a preferential exchange model for inhibition of P/Q-type channels. Finally, the differential occurrence of reluctant openings does not appear to result from distinctions in the rates of $G_{\beta\gamma}$ unbinding, but probably reflects intrinsic differences in the activation pathways of the two channel types.

Here we explore both biophysical and physiological dimensions of the results. First, we consider the implications for basic mechanisms of G-protein inhibition of channels. Second, we critique the data supporting differences in the prevalence of reluctant openings between channel types. Finally, we elaborate on the physiological impact of differential modulation of N- versus P/Q-type channels.

Mechanisms Underlying Differential N- and P/Q-type Channel Modulation

We have argued that the sharp contrast in the prevalence of reluctant openings between N- and P/Q-type channels arises from differences in reluctant mode activation pathways, rather than from differences in the rates of $G_{\beta\gamma}$ dissociation from channels. We inferred that such dissociation rates were similar for voltages ≥30 mV, based on the similarity of time constants for equilibration between willing and reluctant modes of gating (Fig. 10 B). Because the two channel types manifest a clear distinction in the prevalence of reluctant openings over these voltages (Fig. 9), we concluded that this difference was unlikely to arise from differing $G_{\beta\gamma}$ dissociation rates.

It would be reassuring to our conclusion if others had observed the same voltage-dependent pattern of time constants shown in Fig. 10 B. In accord with our results, previous experiments with neurons and heterologous expression systems indicate that facilitation of N- and P/Q-type channels proceeds at similar rates for prepulse voltages ≥100 mV (Currie and Fox, 1997; Meza and Adams, 1998; Roche and Treistman, 1998). By contrast, another study comparing G-protein inhibition of N-type (α_{1B}) and P/Q-type (α_{1A}) channels expressed in *Xenopus* oocytes found that the kinetics of facilitation were consistently about twofold faster for α_{1A} than for α_{1B} over a similar range of prepulse potentials (+60 and 150 mV; Zhang et al., 1996). At more modest depolarizations, the time constant of intermodal exchange has rarely been investigated, in part because of the overlap between the kinetics of slow activation and voltage-dependent inactivation. Here, the use of the calcium-channel β_{2a} subunit dramatically slowed voltage-dependent inactivation (e.g., Jones et al., 1998; Patil et al., 1998), thus facilitating well-resolved exponential fits to the slow phase of current activation at modest voltages. This strategy revealed that over a broad range of more negative voltages, the kinetics of reluctant → willing mode conversion was considerably faster (approximately eightfold faster at −10 mV) for P/Q- compared with N-type channels. Because of the markedly greater voltage dependence of such kinetics in the N-type channel, the time constants for the two channel types converged at more positive voltages. The strong voltage dependence of N-type channel kinetics over a range of modest potentials is in overall agreement with previous analysis in NG108-15 cells (Kasai, 1992). In short, previous results generally support the profile of time constants observed in Fig. 10 B, although this study is the first to explicitly compare the kinetics of N- and P/Q-type channels over such a broad voltage range.

The configuration of time constants for intermodal exchange (Fig. 10 B) bears not only upon potential differences in the activation pathways of N- and P/Q-type channels, but also upon a possible explanation for the lower degree of G-protein inhibition of P/Q-type channels (Mintz and Bean, 1993; Bayliss et al., 1995; Bourinet et al., 1996; Zhang et al., 1996; Currie and Fox, 1997; Roche and Treistman, 1998). The clearly faster time constants for P/Q-type channel facilitation at modest depolarizations point to more rapid $G_{\beta\gamma}$ dissociation, which would result in weaker steady state inhibition, assuming equal association rates between channel types. Zhang et al. (1996) were the first to advance this explanation for the weaker inhibition of P/Q-type channels, but others argued against it based on the similarity of facilitation kinetics at voltages ≥100 mV (Currie and Fox, 1997; Meza and Adams, 1998; Roche and Treistman, 1998). Our observations reconcile the differing perspectives, and support the explanation of Zhang et al. (1996) at moderate potentials with relevance to physiological behavior.

Authenticity of Suggested Differential Prevalence of Reluctant Openings in N- and P/Q-type Channels

A major outcome of this study is the suggestion that the N- but not P/Q-type channel can open in the reluctant mode of gating (reluctant openings). Although the tail G-V experiment and slope-analysis method provide arguably compelling support for this suggestion, the evidence is nevertheless indirect and dependent on several assumptions. We review these assumptions, so as to

gauge the strength of our suggestion and to facilitate comparison with future, more direct experiments.

Regarding the tail G-V experiments (Fig. 4), we mentioned that mechanistic inferences from the 3-ms activation protocol were dependent upon the extent to which intermodal exchange was minimized by the short duration of depolarizing steps. This assumption appears reasonable given that time constants for reluctant → willing mode conversion were at least three- to fourfold longer for voltages up to +50 mV (Fig. 10 B). The assumptions underlying the slope-analysis method are more subtle. First, we postulated that no reluctant openings occurred during the modest 10-mV depolarization in the test pulse (e.g., Fig. 5 A). If this were not true, then the expression for $A_{slow,peak}$, currently given in Eq. 3, should be revised to the form currently applied to $A_{slow,tail}$ (Eq. 6), except that all $P_{o'}(V_{pre})$ terms should be substituted with $P_{o'}(V_{test})$, where V_{test} is the potential during the test pulse. The net result is that the slope we measure (= $A_{slow,tail}$ ÷ modified $A_{slow,peak}$) would underestimate the true slope in the absence of reluctant openings during the test pulse (= $A_{slow,tail}$ ÷ true $A_{slow,peak}$). This would lead to an underestimate in the relative open probability of reluctant channels [$P_{o'}(V_{pre})/P_o(V_{pre})$]. If such underestimates are present to a greater degree in P/Q- versus N-type channels, the inferred difference in the prevalence of reluctant openings could be diminished. However, the results of the tail G-V experiments would still support a strong difference in the prevalence of reluctant openings between channel types. Second, the equations describing activation presume that if reluctant channels can open during a prepulse, their conditional probability of occurrence, given occupancy within the reluctant mode, has reached steady state during the course of the slow phase of activation. If this presumption was false, then the time constants for the slow phases of activation and facilitation would be expected to differ, resulting in nonlinearity that was not apparent in experimentally determined $I_{tail,norm} - I_{peak,norm}$ relations (e.g., Fig. 6 C). Finally, the equations describing activation do not consider the possibility that reluctant openings may manifest a smaller unitary conductance (Kuo and Bean, 1993), although fragmentary single-channel experiments have so far failed to confirm such a difference in unitary conductance (Patil et al., 1996).

While the assumptions underlying our whole-cell analysis seem quite reasonable, the present experiments urgently underscore the need for single-channel experiments to directly establish the core dichotomy in the expression of reluctant openings. In two previous single-channel studies of N-type channels, the major effect of G-protein activation was to delay the time to first opening (Carabelli et al., 1996; Patil et al., 1996), without obvious evidence of reluctant openings. One preliminary study of single N-type channels (Lee and Elmslie, 1997) did report gating consistent with reluctant opening. No comparable studies of single P/Q-type channels have appeared. One drawback of most of these studies, however, is that due to the surface charge screening effects of the high Ba^{2+} concentrations used, the voltages at which G-protein effects were studied corresponded to physiological voltages <0 mV. The voltage dependence of reluctant openings in inhibited N-type channels, as presented here (Fig. 9), makes it clear that detection of single N-type channel reluctant openings would not be expected to occur under the conditions used in the two full-length studies above. As unitary current amplitude diminishes with increasing depolarization, it will be challenging to resolve single-channel events at the positive potentials where appreciable reluctant openings would be predicted. We are, however, encouraged by our preliminary single-channel evidence that reluctant openings can be detected in G-protein–inhibited N-type channels at higher voltages, using quartz pipette technology to aid resolution (Levis and Rae, 1998; Colecraft et al., 1999).

Physiological Implications of Differential Occurrence of Reluctant Openings

N- and P/Q-type channels have been immunocytochemically identified within central and peripheral neurons, and the channels show distinct subcellular locations in dendritic spines, cell bodies, and nerve terminals (Westenbroek et al., 1992, 1998). Using selective toxin blockade of distinct types of calcium channels, complementary studies have focused on the functional contribution of different calcium channels to synaptic transmission at a variety of synapses. Both N-and P/Q-type channels are found to contribute to synaptic transmission, albeit to different degrees in different synapses (Luebke et al., 1993; Takahashi and Momiyama, 1993; Wheeler et al., 1994; Wu and Saggau, 1994; Reid et al., 1998). Some neurons even show the extreme case, where synaptic transmission is entirely mediated by either N- or P/Q-type channels (Poncer et al., 1997). Against this background of variably distributed N- and P/Q-type channels, differential modulation would provide a means to fine tune synaptic transmission tailored to the needs of spatially distinct synapses.

The selective occurrence of reluctant openings at physiologically relevant voltages in N- but not P/Q-type channels represents a new dimension of differential modulation that could contribute to such functional tuning. The presence or absence of reluctant openings during G-protein inhibition could affect the waveform of Ca^{2+} entry during action potentials in fundamentally different ways (Brody et al., 1997). If reluctant openings are not evoked during an action potential, then

G-protein inhibition would simply limit the number of willing channels. In this case, the inhibited waveform of Ca^{2+} entry would preserve its shape, and represent a scaled-down version of the control waveform. By contrast, if both reluctant and willing openings are evoked during an action potential, then the inhibited waveform would reflect the properties of gating transitions surrounding both willing and reluctant open states. One might then predict that the waveform of Ca^{2+} entry during G-protein inhibition would not only be smaller, but altered in shape. Changes in the shape of the Ca^{2+} entry waveform could have substantial physiological consequences for the timing of synaptic transmission (Sabatini and Regehr, 1999). Furthermore, Ca^{2+} influx through a single channel may trigger vesicle release under some conditions (Augustine et al., 1991; Stanley, 1993; Bertram et al., 1996), while multiple channels may contribute in others (Borst and Sakmann, 1998). Alterations in the amplitude and/or shape of the macroscopic Ca^{2+} entry waveform, as well as differences in single-channel open and closed times, may tilt the balance between single- and overlapping-channel regimes of neurotransmitter release, with attendant modulation of synaptic efficacy.

Given the potential functional impact of reluctant openings, it will be critical to determine whether they actually do occur in N-type channels driven by physiological action potentials. Although the present results suggest that such openings occur at physiologically relevant potentials, it remains to be shown whether they can activate fast enough to occur during the brief 1–4-ms duration of action potentials. The outcome will be critically dependent on the first latency of inhibited channels. Future work using action potential waveforms (Brody et al., 1997) will be essential in answering the remaining unknown.

The full extent of the physiological impact of differential G-protein modulation may extend well beyond the simple two-channel dichotomy presented here. For simplicity, we have used only the β_{2a} auxiliary subunit, although there are at least four types of β subunits with multiple splice variants (Perez-Reyes et al., 1992). Different β subunits may impart varying propensities for reluctant opening. Moreover, different splice variants of the various α_{1A} and α_{1B} backbones for N- and P/Q-type channels may also figure in differential G-protein modulation (Lin et al., 1997). For example, an alternatively spliced variant of the P/Q-type (α_{1A}) subunit, termed $\alpha_{1A\text{-}b}$, has been identified. This splice variant differs from the primary sequence of the α_{1A} subunit used here at three sites, one of which is the presence of a single valine insertion in the I–II linker of the new clone (Bourinet et al., 1999). Of particular relevance was the finding that the presence of this valine resulted in currents that were more strongly modulated by G proteins, reminiscent of N-type channel behavior. It will be interesting to determine whether reluctant openings may occur differentially between alternatively spliced variants of the P/Q-type channel.

We thank SIBIA Neurosciences for the human $\alpha_{1B\text{-}1}$ clone, T.P. Snutch for the $\alpha_{1A\text{-}a}$ and $\alpha_{2b}\delta$ clones, E. Perez-Reyes for the β_{2a} clone, Ernst Peralta for the m2 clone, and J.G Mulle and Devi Rathod for technical assistance.

This work was supported by grants from the National Institutes of Health (NIH) (D.T. Yue) and an NIH Medical Scientist Training Program Award (P.G. Patil).

Submitted: 1 October 1999
Revised: 11 January 2000
Accepted: 12 January 2000
Released online: 31 January 2000

REFERENCES

Augustine, G.J., E.M. Adler, and M.P. Charlton. 1991. The calcium signal for transmitter secretion from presynaptic nerve terminals. *Ann. NY Acad. Sci.* 635:365–381.

Bayliss, D.A., M. Umemiya, and A.J. Berger. 1995. Inhibition of N- and P-type calcium currents and the after-hyperpolarization in rat motoneurones by serotonin. *J. Physiol.* 485:635–647.

Bean, B.P. 1989. Neurotransmitter inhibition of neuronal calcium currents by changes in channel voltage dependence. *Nature.* 340: 153–156.

Bertram, R., A. Sherman, and E.F. Stanley. 1996. Single-domain/bound calcium hypothesis of transmitter release and facilitation. *J. Neurophysiol.* 75:1919–1931.

Bito, H., K. Deisseroth, and R.W. Tsien. 1997. Ca^{2+}-dependent regulation in neuronal gene expression. *Curr. Opin. Neurobiol.* 7:419–429.

Boland, L.M., and B.P. Bean. 1993. Modulation of N-type calcium channels in bullfrog sympathetic neurons by luteinizing hormone-releasing hormone: kinetics and voltage dependence. *J. Neurosci.* 13:516–533.

Borst, J.G., and B. Sakmann. 1998. Calcium current during a single action potential in a large presynaptic terminal of the rat brainstem. *J. Physiol.* 506:143–157.

Borst, J.G.G., F. Helmchen, and B. Sakmann. 1995. Pre- and postsynaptic whole-cell recordings in the medial nucleus of the trapezoid body of the rat. *J. Physiol.* 489:825–840.

Bourinet, E., T.W. Soong, A. Stea, and T.P. Snutch. 1996. Determinants of the G protein–dependent opioid modulation of neuronal calcium channels. *Proc. Natl. Acad. Sci. USA.* 93:1486–1491.

Bourinet, E., T.W. Soong, K. Sutton, S. Slaymaker, E. Mathews, A. Monteil, G.W. Zamponi, J. Nargeot, and T.P. Snutch. 1999. Splicing of alpha 1A subunit gene generates phenotypic variants of P- and Q-type calcium channels. *Nat. Neurosci.* 2:407–415.

Brody, D.L., P.G. Patil, J.G. Mulle, T.P. Snutch, and D.T. Yue. 1997. Bursts of action potential waveforms relieve G-protein inhibition of recombinant P/Q-type Ca^{2+} channels in HEK 293 cells. *J. Physiol.* 499:637–644.

Brody, D.L., and D.T. Yue. 1999. Evidence that relief of G-protein inhibition of neuronal calcium channels contributes to short-term synaptic plasticity. *Soc. Neurosci. Abstr.* 25:802. (Abstr.)

Canti, C., K.M. Page, G.J. Stephens, and A.C. Dolphin. 1999. Identification of residues in the N terminus of alpha1B critical for inhibition of the voltage-dependent calcium channel by Gbeta gamma. *J. Neurosci.* 19:6855–6864.

Carabelli, V., M. Lovallo, V. Magnelli, H. Zucker, and E. Carbone.

1996. Voltage-dependent modulation of single N-Type Ca^{2+} channel kinetics by receptor agonists in IMR32 cells. *Biophys. J.* 70:2144–2154.

Colecraft, H.M., D.L. Brody, and D.T. Yue. 1999. Single-channel resolution of reluctant openings in G-protein–inhibited Ca^{2+} channels. *Biophys. J.* 76:A258. (Abstr.)

Currie, K.P., and A.P. Fox. 1997. Comparison of N- and P/Q-type voltage-gated calcium channel current inhibition. *J. Neurosci.* 17: 4570–4579.

De Waard, M., H. Liu, D. Walker, V.E. Scott, C.A. Gurnett, and K.P. Campbell. 1997. Direct binding of G-protein betagamma complex to voltage-dependent calcium channels. *Nature.* 385:446–450.

Dittman, J.S., and W.G. Regehr. 1996. Contributions of calcium-dependent and calcium-independent mechanisms to presynaptic inhibition at a cerebellar synapse. *J. Neurosci.* 16:1623–1633.

Elmslie, K.S., W. Zhou, and S.W. Jones. 1990. LHRH and GTP-gamma-S modify calcium current activation in bullfrog sympathetic neurons. *Neuron*. 5:75–80.

Forscher, P., and G. Oxford. 1985. Modulation of calcium channels by norepinephrine in internally dialyzed avian sensory neurons. *J. Gen. Physiol*. 85:743–763.

Furukawa, T., R. Miura, Y. Mori, M. Strobeck, K. Suzuki, Y. Ogihara, T. Asano, R. Morishita, M. Hashii, H. Higashida, et al. 1998a. Differential interactions of the C terminus and the cytoplasmic I-II loop of neuronal Ca^{2+} channels with G-protein alpha and beta gamma subunits. II. Evidence for direct binding. *J. Biol. Chem.* 273:17595–17603.

Furukawa, T., T. Nukada, Y. Mori, M. Wakamori, Y. Fujita, H. Ishida, K. Fukuda, S. Kato, and M. Yoshii. 1998b. Differential interactions of the C terminus and the cytoplasmic I-II loop of neuronal Ca^{2+} channels with G-protein alpha and beta gamma subunits. I. Molecular determination. *J. Biol. Chem.* 273:17585–17594.

Grassi, F., and H.D. Lux. 1989. Voltage-dependent GABA-induced modulation of calcium currents in chick sensory neurons. *Neurosci. Lett.* 105:113–119.

Herlitze, S., D.E. Garcia, K. Mackie, B. Hille, and W.A. Catterall. 1996. Modulation of Ca^{2+} channels by G-protein beta-gamma subunits. *Nature*. 380:258–262.

Hille, B. 1992. G protein–coupled mechanisms and nervous signaling. *Neuron*. 9:187–195.

Hille, B. 1994. Modulation of ion-channel function by G-protein–coupled receptors. *Trends Neurosci*. 17:531–536.

Ikeda, S.R. 1996. Voltage-dependent modulation of N-type calcium channels by G-protein beta-gamma subunits. *Nature.* 380:255–258.

Ikeda, S.R., and G.G. Schofield. 1989. Somatostatin blocks a calcium current in rat sympathetic ganglion neurones. *J. Physiol.* 409:221–240.

Jones, L.P., P.G. Patil, T.P. Snutch, and D.T. Yue. 1997. G-protein modulation of N-type calcium channel gating current in human embryonic kidney cells (HEK 293). *J. Physiol.* 498:601–610.

Jones, L.P., S.K. Wei, and D.T. Yue. 1998. Mechanism of auxiliary subunit modulation of neuronal α_{1E} calcium channels. *J. Gen. Physiol.* 112:125–143.

Jones, S.W., and K.S. Elmslie. 1997. Transmitter modulation of neuronal calcium channels. *J. Membr. Biol.* 155:1–10.

Kasai, H. 1992. Voltage- and time-dependent inhibition of neuronal calcium channels by a GTP-binding protein in a mammalian cell line. *J. Physiol.* 448:189–209.

Kuo, C.C., and B. Bean. 1993. G-protein modulation of ion permeation through N-type calcium channels. *Nature*. 365:258–262.

Lee, H.K., and K.S. Elmslie. 1997. Characterization of N-channel gating recorded in the presence of norepinephrine. *Soc. Neurosci. Abstr.* 23:856. (Abstr.)

Levis, R.A., and J.L. Rae. 1998. Low-noise patch-clamp techniques. *Methods Enzymol.* 293:218–266.

Lin, Z., S. Haus, J. Edgerton, and D. Lipscombe. 1997. Identification of functionally distinct isoforms of the N-type Ca^{2+} channel in rat sympathetic ganglia and brain. *Neuron*. 18:153–166.

Lipscombe, D., S. Kongsamut, and R. Tsien. 1989. Alpha-adrenergic inhibition of sympathetic neurotransmitter release mediated by modulation of N-type calcium-channel gating. *Nature.* 340: 639–642.

Luebke, J.I., and K. Dunlap. 1994. Sensory neuron N-type calcium currents are inhibited by both voltage-dependent and -independent mechanisms. *Pflügers Arch.* 428:499–507.

Luebke, J.I., K. Dunlap, and T. Turner. 1993. Multiple calcium channel types control glutamatergic synaptic transmission in the hippocampus. *Neuron*. 11:895–902.

Marchetti, C., E. Carbone, and H.D. Lux. 1986. Effects of dopamine and noradrenaline on Ca channels of cultured sensory and sympathetic neurons of chick. *Pflügers Arch.* 406:104–111.

Meza, U., and B. Adams. 1998. G-protein–dependent facilitation of neuronal alpha1A, alpha1B, and alpha1E Ca channels. *J. Neurosci.* 18:5240–5252.

Miller, R.J. 1990. Receptor-mediated regulation of calcium channels and neurotransmitter release. *FASEB J.* 4:3291–3299.

Mintz, I.M., and B.P. Bean. 1993. GABAB receptor inhibition of P-type Ca^{2+} channels in central neurons. *Neuron*. 10:889–898.

Patil, P.G., D.L. Brody, and D.T. Yue. 1998. Preferential closed-state inactivation of neuronal calcium channels. *Neuron*. 20:1027–1038.

Patil, P.G., M. de Leon, R.R. Reed, S. Dubel, T.P. Snutch, and D.T. Yue. 1996. Elementary events underlying voltage-dependent G-protein inhibition of N-type calcium channels. *Biophys. J.* 71: 2509–2521.

Peralta, E.G., A. Ashkenazi, J.W. Winslow, D.H. Smith, J. Ramachandran, and D.J. Capon. 1987. Distinct primary structures, ligand-binding properties and tissue-specific expression of four human muscarinic acetylcholine receptors. *EMBO (Eur. Mol. Biol. Organ.) J.* 6:3923–3929.

Perez-Reyes, E., A. Castellano, H.S. Kim, P. Bertrand, E. Baggstrom, A.E. Lacerda, X.Y. Wei, and L. Birnbaumer. 1992. Cloning and expression of a cardiac/brain beta subunit of the L-type calcium channel. *J. Biol. Chem.* 267:1792–1797.

Poncer, J.C., R.A. McKinney, B.H. Gahwiler, and S.M. Thompson. 1997. Either N- or P-type calcium channels mediate GABA release at distinct hippocampal inhibitory synapses. *Neuron*. 18: 463–472.

Qin, N., D. Platano, R. Olcese, E. Stefani, and L. Birnbaumer. 1997. Direct interaction of $G\beta\gamma$ with a C-terminal $G\beta\gamma$-binding domain of the Ca^{2+} channel alpha1 subunit is responsible for channel inhibition by G protein–coupled receptors. *Proc. Natl. Acad. Sci. USA.* 94:8866–8871.

Reid, C.A., J.M. Bekkers, and J.D. Clements. 1998. N- and P/Q-type Ca^{2+} channels mediate transmitter release with a similar cooperativity at rat hippocampal autapses. *J. Neurosci.* 18:2849–2855.

Roche, J.P., and S.N. Treistman. 1998. The Ca^{2+} channel beta3 subunit differentially modulates G-protein sensitivity of alpha1A and alpha1B Ca^{2+} channels. *J. Neurosci.* 18:878–886.

Sabatini, B.L., and W.G. Regehr. 1999. Timing of synaptic transmission. *Annu. Rev. Physiol.* 61:521–542.

Stanley, E.F. 1993. Single calcium channels and acetylcholine release at a presynaptic nerve terminal. *Neuron*. 11:1007–1011.

Stea, A., W.J. Tomlinson, T.W. Soong, E. Bourinet, S.J. Dubel, S.R. Vincent, and T.P. Snutch. 1994. Localization and functional properties of a rat brain alpha 1A calcium channel reflect similarities to neuronal Q- and P-type channels. *Proc. Natl. Acad. Sci. USA.* 91:10576–10580.

Takahashi, T., and A. Momiyama. 1993. Different types of calcium channels mediate central synaptic transmission. *Nature.* 366:156–158.

Tomlinson, W.J., A. Stea, E. Bourinet, P. Charnet, J. Nargeot, and T.P. Snutch. 1993. Functional properties of a neuronal class C L-type calcium channel. *Neuropharmacology.* 32:1117–1126.

Tsien, R.W., and R.Y. Tsien. 1990. Calcium channels, stores, and oscillations. *Annu. Rev. Cell Biol.* 6:715–760.

Wanke, E., A. Ferroni, A. Malgaroli, A. Ambrosini, T. Pozzan, and J. Meldolesi. 1987. Activation of a muscarinic receptor selectively inhibits a rapidly inactivated Ca^{2+} current in rat sympathetic neurons. *Proc. Natl. Acad. Sci. USA.* 84:4313–4317.

Westenbroek, R.E., J.W. Hell, C. Warner, S.J. Dubel, T.P. Snutch, and W.A. Catterall. 1992. Biochemical properties and subcellular distribution of an N-type calcium channel alpha 1 subunit. *Neuron.* 9:1099–1115.

Westenbroek, R.E., L. Hoskins, and W.A. Catterall. 1998. Localization of Ca^{2+} channel subtypes on rat spinal motor neurons, interneurons, and nerve terminals. *J. Neurosci.* 18:6319–6330.

Wheeler, D.B., A. Randall, and R.W. Tsien. 1994. Roles of N-type and Q-type Ca^{2+} channels in supporting hippocampal synaptic transmission. *Science.* 264:107–111.

Williams, M.E., P.F. Brust, D.H. Feldman, S. Patthi, S. Simerson, A. Maroufi, A.F. McCue, G. Velicelebi, S.B. Ellis, and M.M. Harpold. 1992. Structure and functional expression of an omega-conotoxin-sensitive human N-type calcium channel. *Science.* 257:389–395.

Wu, L.G., and P. Saggau. 1994. Adenosine inhibits evoked synaptic transmission primarily by reducing presynaptic calcium influx in area CA1 of hippocampus. *Neuron.* 12:1139–1148.

Wu, L.G., and P. Saggau. 1997. Presynaptic inhibition of elicited neurotransmitter release. *Trends Neurosci.* 20:204–212.

Zamponi, G.W., E. Bourinet, D. Nelson, J. Nargeot, and T.P. Snutch. 1997. Crosstalk between G proteins and protein kinase C mediated by the calcium channel alpha1 subunit. *Nature.* 385: 442–446.

Zamponi, G.W., and T.P. Snutch. 1998. Decay of prepulse facilitation of N type calcium channels during G protein inhibition is consistent with binding of a single G beta subunit. *Proc. Natl. Acad. Sci. USA.* 95:4035–4039.

Zhang, J.-F., P.T. Ellinor, R.W. Aldrich, and R.W. Tsien. 1996. Multiple structural elements in voltage-dependent Ca^{2+} channels support their inhibition by G proteins. *Neuron.* 17:991–1003.

Zhu, Y., and S.R. Ikeda. 1994. VIP inhibits N-type Ca^{2+} channels of sympathetic neurons via a pertussis toxin–insensitive but cholera toxin–sensitive pathway. *Neuron.* 13:657–669.